AD

USAAVLABS TECHNICAL REPORT 66-86

DEVELOPMENT OF EQUIPMENT AND TECHNIQUES FOR COMPLEX FATIGUE LOADING

By

Herbert Kartluke
Philip G. Luckhardt
Gary D. Pruder

December 1966

U. S. ARMY AVIATION MATERIEL LABORATORIES
FORT EUSTIS, VIRGINIA

CONTRACT DA 44-177-AMC-257(T)
AEROPROJECTS INCORPORATED
WEST CHESTER, PENNSYLVANIA

Disclaimers

The findings in this report are not to be construed as an official Department of the Army position unless so designated by other authorized documents.

When Government drawings, specifications, or other data are used for any purpose other than in connection with a definitely related Government procurement operation, the United States Government thereby incurs no responsibility nor any obligation whatsoever; and the fact that the Government may have formulated, furnished, or in any way supplied the said drawings, specifications, or other data is not to be regarded by implication or otherwise as in any manner licensing the holder or any other person or corporation, or conveying any rights or permission, to manufacture, use, or sell any patented invention that may in any way be related thereto.

Trade names cited in this report do not constitute an official endorsement or approval of the use of such commercial hardware or software.

Disposition Instructions

Destroy this report when no longer needed. Do not return it to originator.

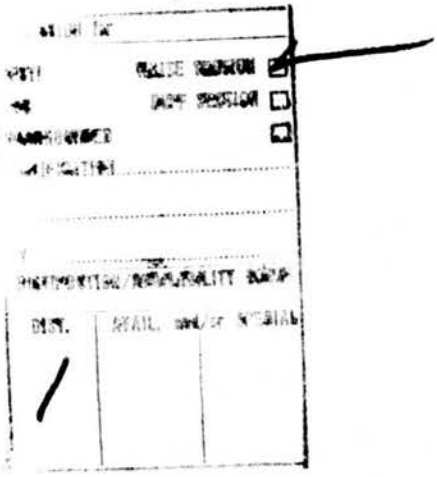

DEPARTMENT OF THE ARMY
U. S. ARMY AVIATION MATERIEL LABORATORIES
FORT EUSTIS, VIRGINIA 23604

This program was performed under Contract DA 44-177-AMC-257(T) with Aeroprojects Incorporated.

The data contained in this report demonstrate the feasibility of fatigue testing with simultaneous application of high-frequency, low-frequency, and static loading to a test specimen.

This report has been reviewed by the U.S. Army Aviation Materiel Laboratories and is considered to be technically sound.

Task 1P125901A17002
Contract DA 44-177-AMC-257(T)
USAAVLABS Technical Report 66-86
December 1966

DEVELOPMENT OF EQUIPMENT AND TECHNIQUES FOR COMPLEX FATIGUE LOADING

by

Herbert Kartluke
Philip G. Luckhardt
Gary D. Pruder

Prepared by

AEROPROJECTS INCORPORATED
WEST CHESTER, PENNSYLVANIA

for

U. S. ARMY AVIATION MATERIEL LABORATORIES
FORT EUSTIS, VIRGINIA

SUMMARY

Fatigue testing apparatus for simultaneous application of high-frequency, low-frequency, and static loading was designed and constructed. The equipment provided for the introduction of high-frequency vibratory energy at 15,000 cycles per second at one end of a specimen and static loading and low-frequency vibration at 2000 cycles per minute at the opposite end. Specimens with a necked-down test section were designed for resonance at the high frequency, and the specimen holding arrangement insured effective delivery of the high-frequency energy into the specimen.

The feasibility of the apparatus as a fatigue test instrument was demonstrated in limited tests on integral specimens of 4340 steel, 2014-T6 aluminum alloy, and 6Al-4V titanium alloy, and on joint specimens of 4340 steel involving fusion-welded, riveted, adhesive-bonded, and brazed joints. With constant low-frequency and static loads, the specimens generally demonstrated shorter elapsed time to failure as the high-frequency power input was increased. The titanium alloy, however, appeared to be insensitive to the high-frequency vibration at the power levels used, possibly because of its internal hysteresis characteristics.

The equipment provides a means for laboratory testing of materials and joint designs for knowledge of materials behavior under conditions encountered in rocket-propelled vehicles. It was recommended that comprehensive fatigue testing be carried out with this apparatus and that methodology be evolved for evaluation and use of the test data.

FOREWORD

This report covers the work accomplished in Phase I of an extended program of development of equipment and techniques for high-frequency vibratory testing. The report was prepared by Aeroprojects Incorporated, West Chester, Pennsylvania, under Army Contract No DA 44-177-AMC-257(T). Dr. Robert L. Echols, Chief, Physical Sciences Laboratories Division, U. S. Army Aviation Materiel Laboratories, Fort Eustis, Virginia, served as Project Officer.

BLANK PAGE

TABLE OF CONTENTS

	Page
SUMMARY	iii
FOREWORD	v
LIST OF ILLUSTRATIONS	ix
LIST OF TABLES	x
INTRODUCTION	1
STATE-OF-THE-ART LITERATURE REVIEW ON HIGH-FREQUENCY FATIGUE TESTING	3
SPECIMEN DESIGN AND FABRICATION	5
Joint Specimens	7
Specimen End Reinforcement	9
FATIGUE LOADING APPARATUS	12
Machine Framework	12
Static Loading System	12
Low-Frequency System	15
High-Frequency System	17
Specimen Mounting	17
Temperature and Atmosphere Control	20
INSTRUMENTATION AND DETERMINATION OF VARIABLES	21
Static Load	21
Static and Low-Frequency Stresses	21
High-Frequency Power	22
High-Frequency Displacement Amplitude	22
Specimen Temperature	23
Number of Cycles to Failure	25
DEMONSTRATION OF FEASIBILITY	26
Material Performance	26
Steel Specimens	29
Aluminum Alloy Specimens	29
Titanium Alloy Specimens	34

TABLE OF CONTENTS (Concluded)

	Page
Joint Performance	36
Welded Specimens	40
Riveted Specimens	40
Adhesive-Bonded Specimens	40
Brazed Specimens	41
EVALUATION OF EQUIPMENT AND CONCLUSIONS	42
RECOMMENDATIONS	44
BIBLIOGRAPHY	45
APPENDIX I, CHRONOLOGICAL LITERATURE REVIEW ON HIGH-FREQUENCY FATIGUE TESTING	46
APPENDIX II, DESIGN OF SAMPLE CONFIGURATION	59
APPENDIX III, FORCE-INSENSITIVE MOUNTING SYSTEM	62
DISTRIBUTION	65

ILLUSTRATIONS

Figure		Page
1	Test Specimen Configuration	8
2	Typical Riveted Joint Pattern for Fatigue Test Specimen .	9
3	Geometry of Doubler Attachments to Test Specimens	11
4	Fatigue Test Apparatus and Associated Instrumentation . .	13
5	Schematic Representation of Fatigue Loading Apparatus . .	14
6	Low-Frequency System Mounted Below Lower Main Plate . . .	16
7	High-Frequency Vibratory System Mounted on Upper Main Plate	16
8	Design of Specimen-Holding Jaws	18
9	Specimens Mounted in Clamping Jaws	19
10	Typical Calibration Curves of Vibratory Displacement vs. Crystal Output at Upper and Lower Clamping Jaws	24
11	Representative Oscillograph of Strain Gage Output	28
12	Effect of High-Frequency Vibration on Fatigue Life of Integral Specimens	31
13	Effect of High-Frequency Stressing on Specimen Temperature and Rate of Temperature Rise for 4340 Steel	32
14	Typical Fatigue Failures of Specimens Under Combined Static, Low-Frequency, and High-Frequency Loading	33
15	Power Loss and Strain Characteristics of Candidate Coupler Materials at 15 Kilocycles per Second	35
16	Effect of High-Frequency Vibration on Fatigue Life of Joint Specimens of 4340 Steel	38
17	Force-Insensitive Mounting Device	67

TABLES

Table		Page
I	Materials Data for Fatigue Test	6
II	Loading Conditions for Integral Specimens	27
III	Test Data for Integral Specimens	30
IV	Loading Conditions for Joint Specimens of 4340 Steel . .	36
V	Test Data for Joint Specimens of 4340 Steel	37

INTRODUCTION

The objectives of this work were to:

1. Establish the present state of the technology in high-frequency fatigue testing and material properties.

2. Provide a compound fatigue loading apparatus capable of simultaneously applying high-frequency loading, normal-frequency loading, and static loading.

3. Provide instrumentation to study high-frequency, static, and low-frequency loading.

4. Establish the feasibility of the system for testing materials and assembled joints.

5. Analyze the results and evaluate the effectiveness of the equipment for fatigue testing.

Conventional fatigue tests are carried out at low frequencies ranging from a few hundred to a few thousand cycles per minute. These frequencies adequately simulate the vibration encountered with most land-operated equipment, such as machinery or automotive apparatus. In jet and rocket engines, the combustion process emits high-intensity acoustic waves at both sonic and ultrasonic frequencies. For example, a 5000-pound-thrust jet engine can have a sound spectrum ranging from 30 cycles per second to well over 10,000 cycles per second (reference 9). These sound waves penetrate all parts of the vehicle, which may be carrying substantial static loads, and act to produce widely varying cyclic amplitudes throughout the structure. The vibratory amplitude may be increased drastically due to resonance of discrete parts of the structure. Performance of the materials and structures is thereby influenced, and in some instances fatigue failure can occur.

Substantial work is currently being done in sonic fatigue test facilities (reference 1) to simulate service loading conditions. High noise levels are generated usually by jet engines, sirens, or loud speakers, operating either at a discrete frequency or over a broad frequency spectrum which, in a few instances, covers the range up to 10,000 cycles per second, but rarely higher. Since the generated sound is nearly always airborne, it is exceedingly difficult to control the stress imposed on, or the strain induced in, the specimen or structure. Such control can best be achieved by direct coupling of the specimen to a controllable source of vibratory energy, as in conventional fatigue measurements.

At the outset of this investigation, the available literature, both domestic and foreign, was reviewed. Reported efforts along this line appear not to have been carried beyond the laboratory stage, and investigators have recognized the difficulties in transmitting significant amounts of high-frequency vibratory energy into test specimens. Moreover, the available literature exhibited no indications that high-frequency fatigue loading had been combined with static and/or low-frequency loading.

The equipment evolved in the present work goes well beyond the apparatus utilized by previous investigators: It provides for the simultaneous application of three discrete types of loading. It includes a mounting method for the high-frequency energy source so that losses to the support structure are negligible, and significant and controllable amounts of energy can be transmitted into the specimen.

The high-frequency system consisted of an ultrasonic transducer-coupling system operating at a nominal frequency of 15,000 cycles per second. Low-frequency loading was applied with a mechanical device comprising counterrotating eccentrically loaded disks. Static biasing loads were applied via pneumatic cylinders connected to a high-pressure nitrogen cylinder.

A sophisticated specimen configuration, compatible with both mounting and joint requirements, providing response and performance characteristics suitable for fatigue evaluation, and designed to be resonant at the high frequency, was developed.

To demonstrate the feasibility of the system, a limited number of specimens were cyclically loaded to failure. The results were encouraging; sensitivity to high-frequency input was shown in steel specimens and relative insensitivity in titanium alloy specimens. The potential findings concerning internal hysteresis characteristics of a material or a joint by this procedure suggest that the system may be a valuable tool for the comparative evaluation of structural configurations.

STATE-OF-THE-ART LITERATURE REVIEW ON HIGH-FREQUENCY FATIGUE TESTING

Review of the literature (presented in detail in Appendix I) indicates sporadic interest for a number of years in high-frequency vibratory testing of materials as a means of accelerating conventional fatigue testing. Limited experimental work has been carried out in the United States, England, France, Germany, Japan, and Russia.

Most of the effort to date in this direction has been on a laboratory scale, oriented to developing high-frequency equipment, obtaining preliminary data for selected materials, attempting comparisons of high-frequency with low-frequency test results, or merely evaluating the behavior of materials.

Various types of systems have been used to generate the high-frequency vibration. Some of the earlier devices were pneumatic resonance, electromagnetic, or electrodynamic vibrators, which were restricted as to the maximum frequency obtainable (generally below about 4000 cycles per second, although somewhat higher in some instances). Most of the more recent work has utilized transducer-coupling systems incorporating magnetostrictive, piezoelectric, or electrostrictive transducers, and generally operating at frequencies in the range of 15,000 to 25,000 cycles per second.

The use of frequencies above about 5000 cycles per second was first suggested in 1932 (reference 4), but it was not until 1950 (reference 7) that practical apparatus for this purpose was evolved. The arrangement then described by Mason, consisting of a transducer driving through a shaped coupler (to amplify the vibratory displacement) into a dumbbell-shaped specimen, became the general design used by most subsequent investigators. Mason used his array, not to determine fatigue life, but rather to examine the behavior of metallic materials during stressing to failure. Others used equipment of this type for determining the fatigue life of materials.

The advantages of high-frequency fatigue as a replacement for conventional (low-frequency) tests have been variously reported to include the greatly increased speed of testing, the possibility of extending such tests beyond the present limit of about 10^9 cycles, the economy and ease of operation, the absence of moving parts, and the absence of noise.

However, correlation of the high-frequency with the low-frequency results is recognized to be a problem. In some instances fatigue life (in number of cycles) was significantly extended at high frequencies; in others the fatigue limit at a given number of cycles was increased.

One investigator (reference 3) found no significant difference in results at 60 cycles per second and at 17,500 cycles per second, although he recognised that the high-frequency vibratory amplitudes achieved in the specimens with his equipment array were small.

It is significant that all of the reported work involved cyclic stressing of the specimens only in axial tension-compression. In no instance was the high-frequency excitation superimposed on a static load to produce cyclic stress in tension-tension, nor was high-frequency superimposed on low-frequency stressing. Apparently no high-frequency system has been used to evaluate fatigue in bending, torsion, or other modes. Except for limited experimentation with simulated turbine blades, the technique has not been applied to actual components or assemblies, but only to materials. Thus there remain broad areas for further experimentation in the field.

SPECIMEN DESIGN AND FABRICATION

The test specimen requirements were dictated by consideration of material properties in conjunction with anticipated static and low-frequency load levels. In addition, the specimen and its supports were required to respond appropriately to the high frequency, with an elastic standing wave in the specimen locale being evaluated. Appendix II presents an analysis of the relationship between critical dimensions of the specimen to concentrate the high-frequency cyclic stress at the center of the specimen. For convenience, this relationship was evolved for cylindrical specimens; its pertinence to a flat-sheet configuration is evident.

This analysis indicates that the test section of the specimen should have a length equal to one half-wavelength at the frequency of operation (15,000 cycles per second) in the material comprising the specimen, and that the overall length of the specimen, due to practical considerations, should be equal to three half-wavelengths.

Three specimen materials were selected for evaluation of the fatigue apparatus: AISI 4340 steel, 2014-T6 aluminum alloy, and 6Al-4V titanium alloy. Pertinent properties of these materials are presented in Section A of Table I.

Consideration was given to the requirements for static, low-frequency, and high-frequency loading of specimens of the above design, which would provide guidance for design of the fatigue apparatus.

Section B of Table I shows the static force required to stress a specimen of each material to its yield point. Although such a magnitude of static stress was not contemplated for this work, these data provided a reasonable load factor for machine design that would permit testing larger specmens or specimens made of higher strength materials. The requirements for a static force-application system to apply such loads are also delineated.

The design conditions for the low-frequency loading system are summarized in Section C of Table I. These conditions were based on the use of counterrotating weights capable of cyclically loading the specimen to one-half their yield strength. A rotational speed of 2000 rpm, providing low-frequency stressing at about 2000 cycles per minute, was selected. The radius arm and eccentric mass were calculated to provide the required loading at this rotational speed.

The conditions for high-frequency loading in Section E of Table I are based on information previously obtained in our laboratory (reference 6) for the steel and titanium alloy. Comparable information was not available for the aluminum alloy, but the requirements for this material are substantially less stringent. The data were computed for an operating frequency of 15,000 cycles per second.

TABLE I

MATERIALS DATA FOR FATIGUE TEST

	Property and Unit	4340 Steel, Normalized	2014-T6 Aluminum Alloy	6Al-4V Titanium Alloy
A. Physical Properties	Ultimate Strength, psi	125,000	67,000	143,000
	Yield Strength, psi	103,000	60,000	136,900
	Young's Modulus, psi	30.8×10^6	10.2×10^6	16.5×10^6
	Sound Velocity, m/sec	5,200	5,000	5,080
	Density, gm/cc	7.85	2.80	4.43
B. Static	Force to Yield, lb	6,030	3,515	8,020
	Piston Gas Pressure, psi	200	200	200
	Cylinder Diameter, in.	5.50	4.13	6.33
C. Low-Frequency	Stress, psi	±51,500	±30,000	±68,450
	Force, lb	3,015	1,708	4,010
	Rotation Rate, rpm	2,000	2,000	2,000
	Radius Arm, in.	3.28	1.86	4.36
	Eccentric Mass, lb	8.1	8.1	8.1
D. High-Frequency	Fatigue Strain, in./in.	0.7×10^{-3}	-	1.45×10^{-3}
	Fatigue Stress, psi*	±21,560	-	±23,925
	Max. Vibratory Displacement, in.	1.52×10^{-3}	-	3.08×10^{-3}
	Power Loss for Center $\lambda/2$, watts	222	-	209
	Estimated Input Power, watts	850	-	1,000
E. Specimen Dimensions	Total Length, $3\lambda/2$, in.	20.5	19.7	20.0
	Test Section Length, in.	2.0 (min.)	2.0 (min.)	2.0 (min.)
	Width, in.	0.9375	0.9375	0.9375
	Thickness, in.	0.0625	0.0625	0.0625

* Stress calculated on basis of static Young's modulus.

Since the loading conditions delineated in Table I appeared to provide a reasonable basis for design of the fatigue test equipment, this work proceeded on the basis of the considerations presented above; i.e., according to the geometry shown in Figure 1 and having the dimensions in Section E of Table I. The specimen width outside the test area was made approximately 2 inches to preclude failure outside the critical locale of the specimen.

JOINT SPECIMENS

In addition to evaluating response of certain metallic materials to complex loading, the investigation required demonstration of the technique with several types of joints in certain materials. Fusion-welded, riveted, adhesive-bonded, and brazed junctions of 4340 steel were studied.

The requirements of the various types of joints imposed further restrictions on specimen design. In order not to make unreasonable demands on the fatigue equipment, it was desirable to minimize the specimen cross section in the test region. This presented no serious difficulties with the welded, adhesive-bonded, or brazed joints, but the riveted type required consideration of rivet diameter, rivet spacing, and edge distance. Based on the use of 1/8-inch rivets, a pattern consisting of five rivets in two staggered rows was selected, and acceptable dimensions according to AN specifications (reference 8) were established as shown in Figure 2. The width of the test section was thus indicated to be 15/16 inch.

With the exception of the metallurgical joints which were butt-welded, all of the joint specimens were of the single-lap type, although it was recognized that joint eccentricity could induce ancillary modes of high-frequency vibration and significantly affect the performance of such a junction in a resonant standing-wave system.

The welded specimens consisted of two half-sections joined by heli-arc butt welding to achieve a configuration similar to that of the integral specimens. These half-sections were preheated to approximately 350°F over approximately 1-inch lengths from the ends to be welded. Welding was carried out by using an Oxweld 65 welding rod, with a 100-ampere current, and under an argon blanket of 18 cubic feet per hour. The preheated specimens were spaced approximately 1/16 inch apart and welded from both sides to give 100-percent weld penetration.

The riveted joints were fabricated to AN specifications with a single overlap of 9/16 inch, as indicated in Figure 2. These joints incorporated 1/8-inch Monel brazer-head rivets inserted in No. 30 drilled holes (0.1285-inch diameter).

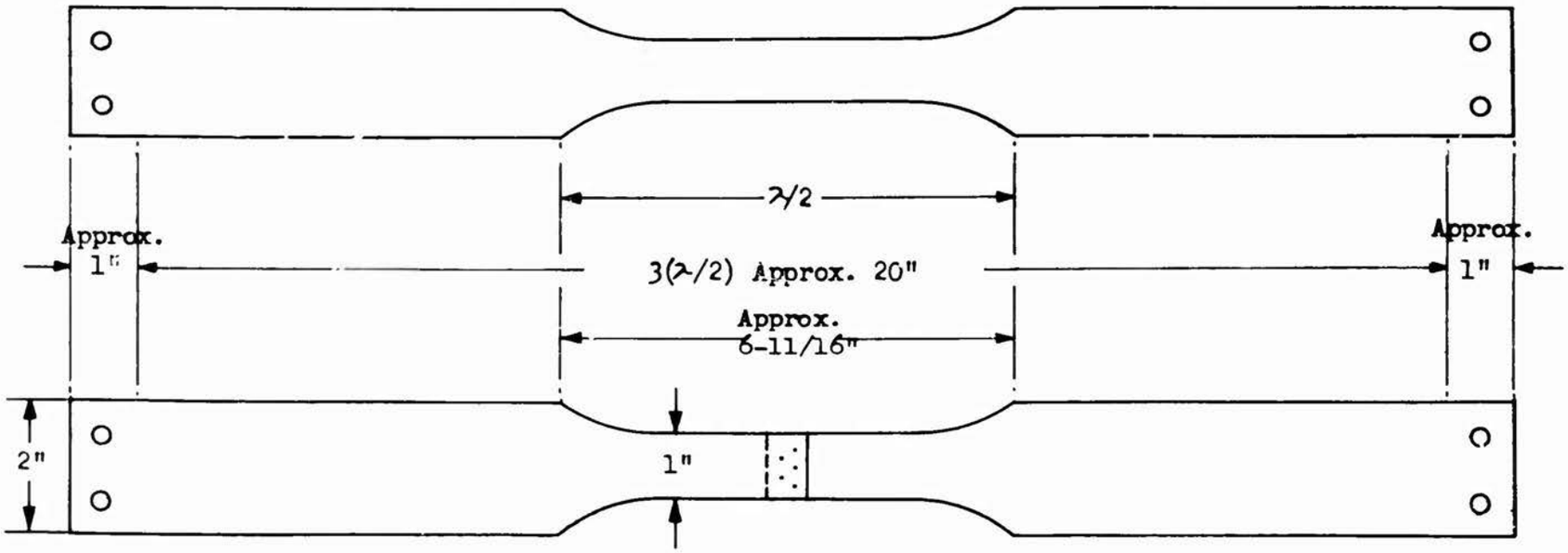

Figure 1. Test Specimen Configuration.

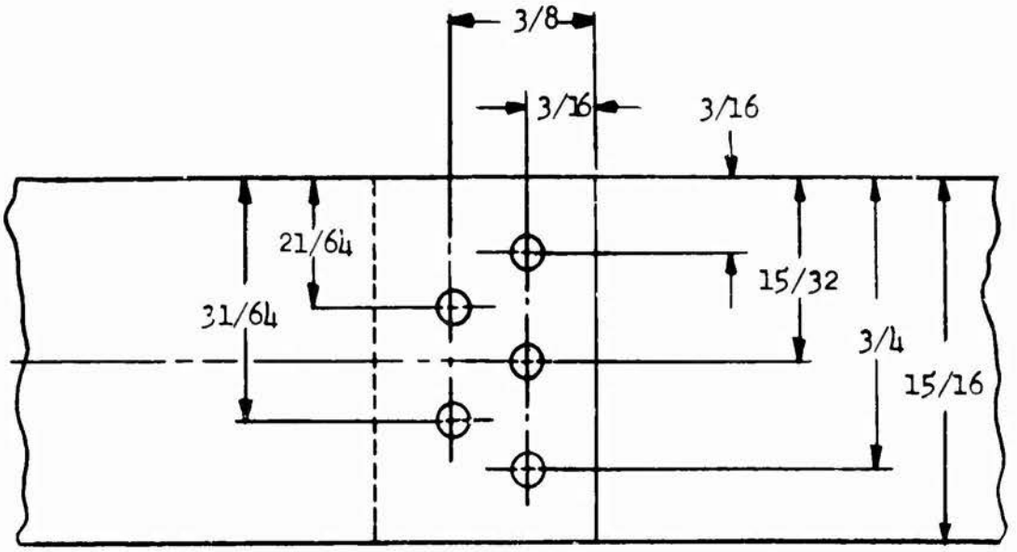

Figure 2. Typical Riveted Joint Pattern for Fatigue Test Specimen. (All dimensions shown are in inches.)

The adhesive-bonded specimens were made of two sections, with a single overlap of 1/2 inch. The overlap areas were cleaned with nitric acid and bonded with EPON-8 epoxy resin. The sections were assembled in a fixture which insured an epoxy thickness after bonding of 0.001 inch. The joints were cured for 1 hour at 150°F.

The brazed specimens were likewise fabricated from two sections, with a single overlap of 1/2 inch. Handy and Harman No. 560 silver solder leaf braze was used, and the joint was fluxed with Handy and Harman B-1 flux. The components were overlapped by 1/2 inch, with the braze leaf at the interface, and then were clamped in a fixture which maintained dimensional control and were heated with an acetylene torch to the melting point of the braze material.

SPECIMEN END REINFORCEMENT

Special consideration was given to design of the junction between the specimen and the machine specimen-holding jaws. This locale was critical, since slip or lack of axial contact of the specimen in the joint would reduce efficiency or even prevent transmission of high-frequency vibratory energy.

To provide the necessary firm contact, the end attachment areas of the specimens incorporated doublers 0.032 inch thick for insertion into precisely machined clevis-type end fittings on the testing machine (described later).

The doubler pads for the steel and aluminum alloy specimens were metallurgically bonded to the specimens as indicated in Figure 3A. However, efforts to braze or solder the doublers to the titanium alloy specimens were unsuccessful. Adhesive bonding of the attachments was unsatisfactory because available adhesives would not develop the shear strength necessary for the static and dynamic loading of the specimens. The arrangement eventually evolved is shown in Figure 3B. It consisted of a mechanical key design with five rivets to carry the tension load across the doubler-specimen interface. Because of the reduction in cross-sectional area and the notching created by the rectangular keyways in these specimens, it became necessary to reduce the specimen cross-sectional area below that indicated in Table I. The reduction was accomplished by grinding the flat surfaces of the titanium specimens while they were bowed.

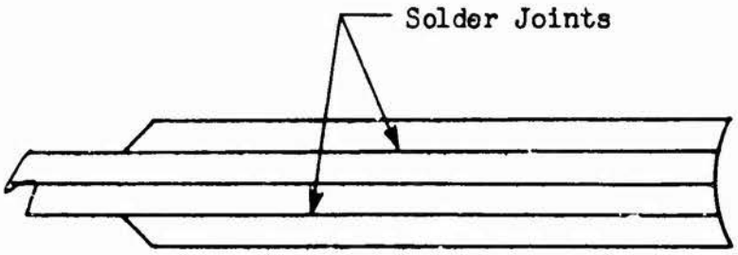

A. Metallurgical Bonding to Steel and Aluminum Alloy Specimens.

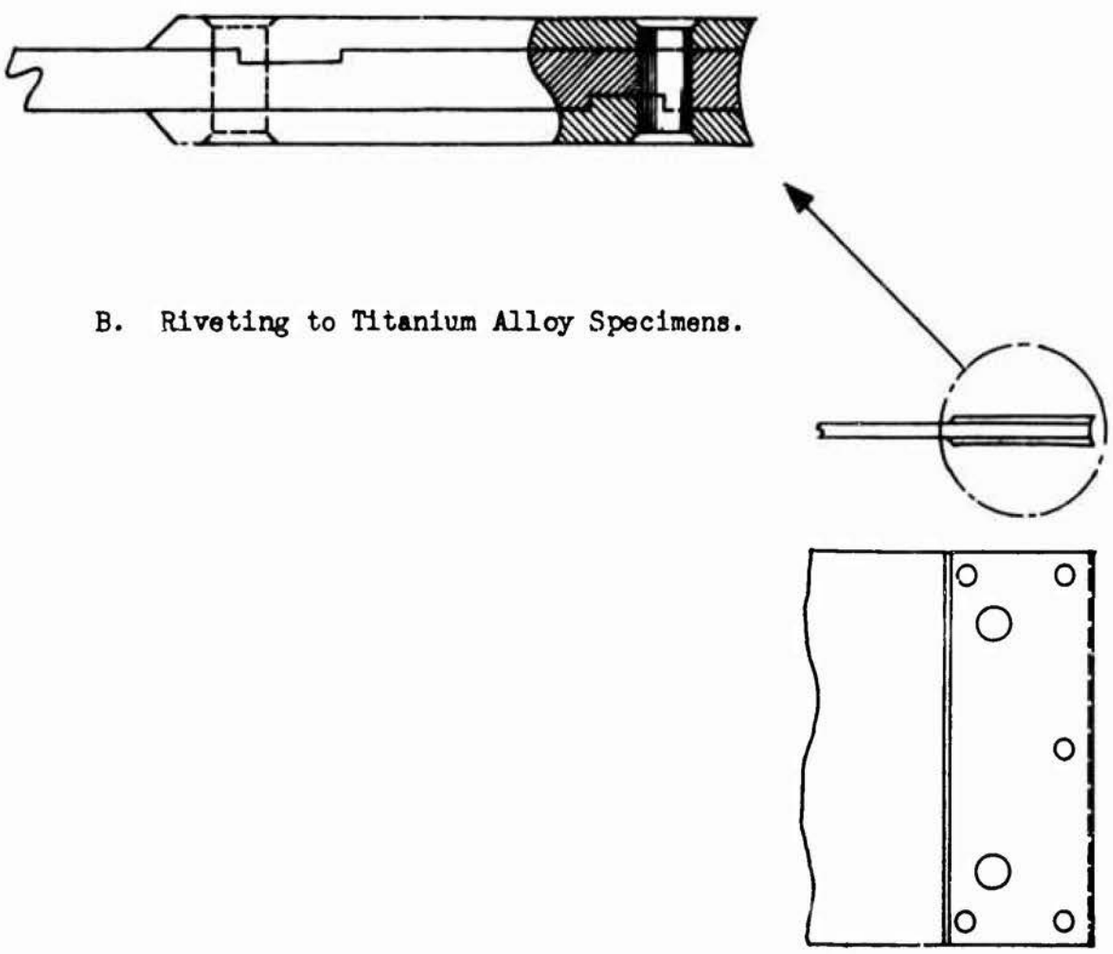

B. Riveting to Titanium Alloy Specimens.

Figure 3. Geometry of Doubler Attachments to Test Specimens.

FATIGUE LOADING APPARATUS

Apparatus for complex loading of the specimens was designed, assembled, and instrumented to obtain information on the behavior of the test specimens under the required complex loading conditions. The complete equipment array with associated instrumentation is illustrated in Figure 4, and the machine design is shown schematically in Figure 5.

MACHINE FRAMEWORK

The framework for the machine was of triangular design, incorporating a lower main plate which supported the static and low-frequency systems and an upper main plate which supported the high-frequency system. The two plates were separated by three precisely machined compression tubes, and the assembly was held together by threaded tension rods having a diameter of 3/4 inch and extending through the compression tubes. The specimens were installed in the area between the main plates, as is evident in Figures 4 and 5.

STATIC LOADING SYSTEM

Mounted through the lower baseplate were two pneumatic cylinders, the piston rods of which were connected, below the plate, to the support for the lower specimen-holding fixture, thus providing a means for statically loading the specimen in tension. Pneumatic, rather than hydraulic, cylinders were chosen for the force application system, since the latter would act as dashpots under the cyclic loading. The cylinders had bores of 3.250 inches, which provided a piston area for the two cylinders of 16.58 square inches. These cylinders were operable at pressures up to 750 psi.

Bottled gas was used as the pressurizing medium to provide pressures high enough to develop the desired levels of static force while operating on the relatively small-bore pistons. The use of compressed air from the plant piping system would have necessitated cylinders of much larger diameter to develop the desired force levels. Nitrogen was chosen as the pressurizing gas to preclude the generation of explosive mixture by reaction of other gases (such as air) with the lubricant. A pressure regulator on the nitrogen bottle insured that the pressure was maintained constant throughout a test.

The static load applied by these cylinders was augmented by the weight of the low-frequency cyclic system located below the lower main plate.

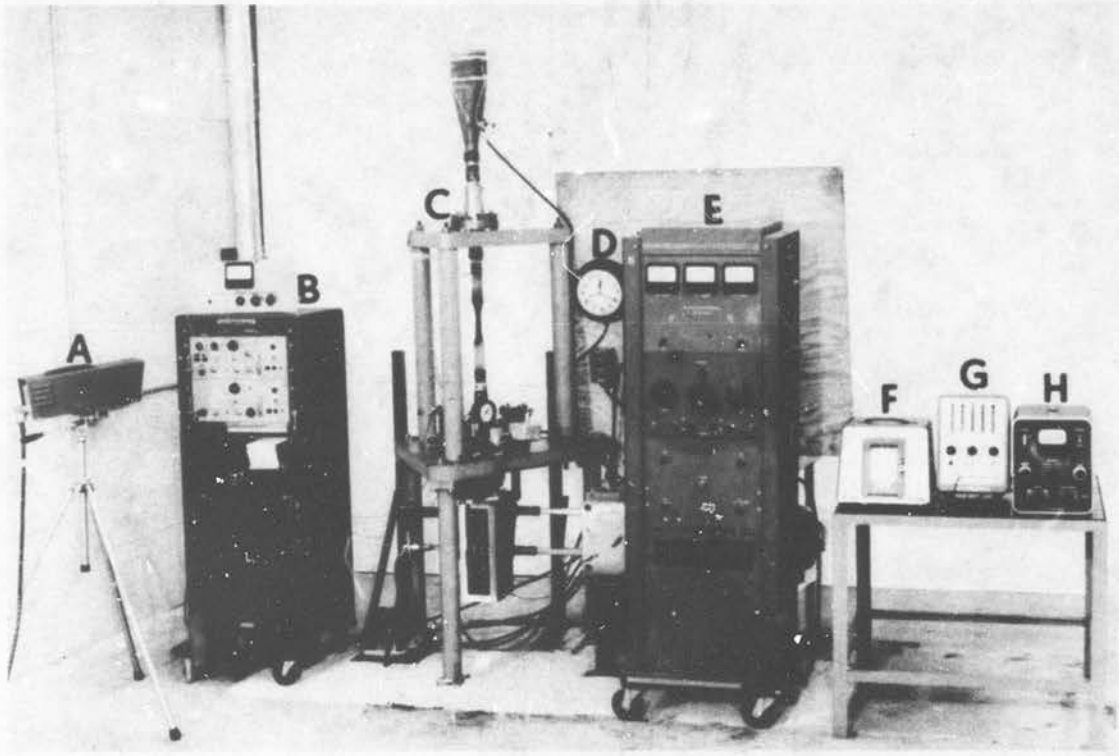

Figure 4. Fatigue Test Apparatus and Associated Instrumentation.

A. Infrared Radiometer.
B. Strip-Chart Recorder for Static and Low-Frequency Loading and for Temperature Indication.
C. Fatigue Apparatus.
D. Electric Timer.
E. Frequency Converter.
F. Strip-Chart Recorder for High-Frequency Displacement.
G. Frequency Counter.
H. Radiometer Control Panel.

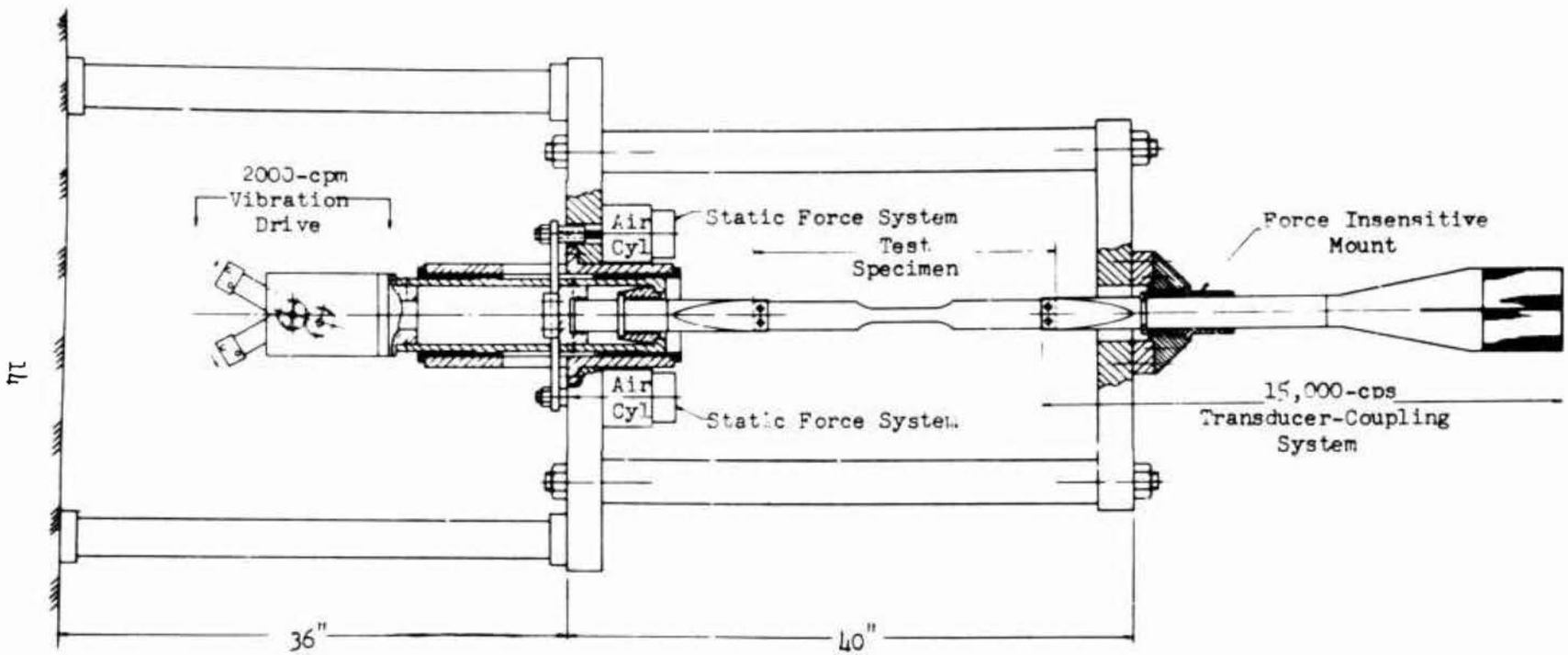

Figure 5. Schematic Representation of Fatigue Loading Apparatus

LOW-FREQUENCY SYSTEM

The low-frequency system, shown in Figure 6, was of conventional design, comprising three counterrotating weighted disks to apply a cyclic reversing load, aligned with the specimen axis, to the support for the lower specimen-holding jaw. The disks had a radius of 5.25 inches and included means for attaching interchangeable copper weights to provide the desired loading of the system. Weights up to 1660 grams were used. A "nutcracker" linkage installed just above the rotating disks and below the lower baseplate maintained alignment of the low-frequency system.

The disks were driven by a 5-horsepower motor rotating at 1735 rpm through a single-ratio reduction gearbox with opposed output shafts, producing speeds of approximately 2000 rpm.

To provide automatic shut-off of the motor on test specimen failure, a switch was installed so that it would be triggered by the drop of the counterrotating assembly upon specimen failure.

During initial operation, the low-frequency cyclic motor would not accelerate above 1180 rpm. Stroboscopic and vibratory examination revealed high-amplitude oscillation of the motor and driving gearbox assembly with reference to the main frame of the equipment at this rotative speed. The motor and gearbox assembly were therefore detached from the main frame and supported from the floor to eliminate coupling between the frame and the motor gearbox assembly. The machine then immediately achieved normal rotative speed of 2000 rpm, but heating of the rotating-mass bearing supports was observed.

In an effort to eliminate such heating, the design of the bearings and support structure was revised to include pressure-lubricated needle bearings instead of the Oilite sleeve bearings. Forced oil circulation was used to insure that excess heat would be carried out of the rotating-mass bearing support assembly.

During one of the early test runs, failure occurred in a spacer disk in this assembly. The failure was traced to the galling of a bronze thrust washer on the shaft carrying the rotating weight disks; bronze chips had worked into one of the needle bearings on this shaft, causing it to skew and eventually to fail. The middle bearing inner races, which were originally integral with the rotating shaft, were then machined to allow insertion of a hardened steel sleeve. Due to the marginal shaft size, the hardened steel inner races were maintained at minimum thickness. Initial operation with this arrangement resulted in fracture and cracking of the hardened steel races.

The complete system of counterrotating weight disks, supports and bearings was therefore redesigned to incorporate larger bearings having a

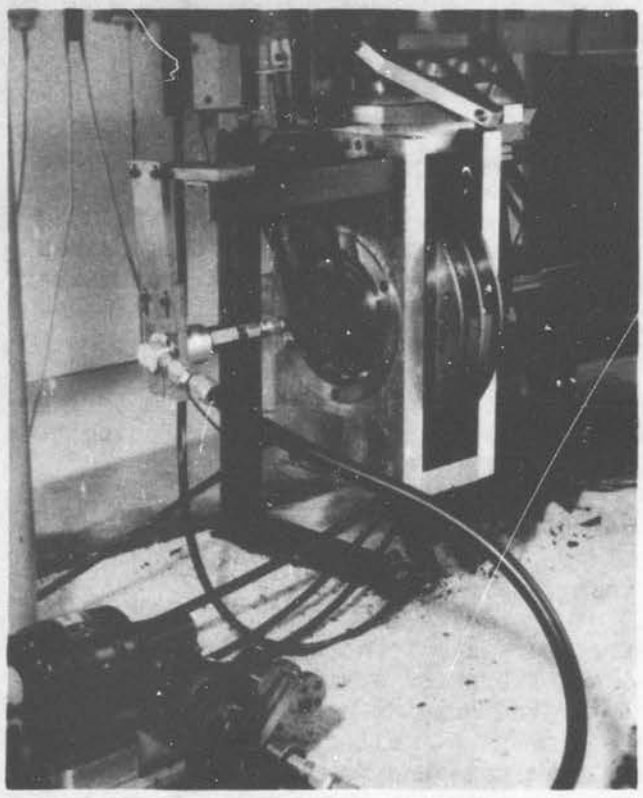

Figure 6. Low-Frequency System Mounted Below Lower Main Plate.
(Pressure lubrication pump at lower left.)

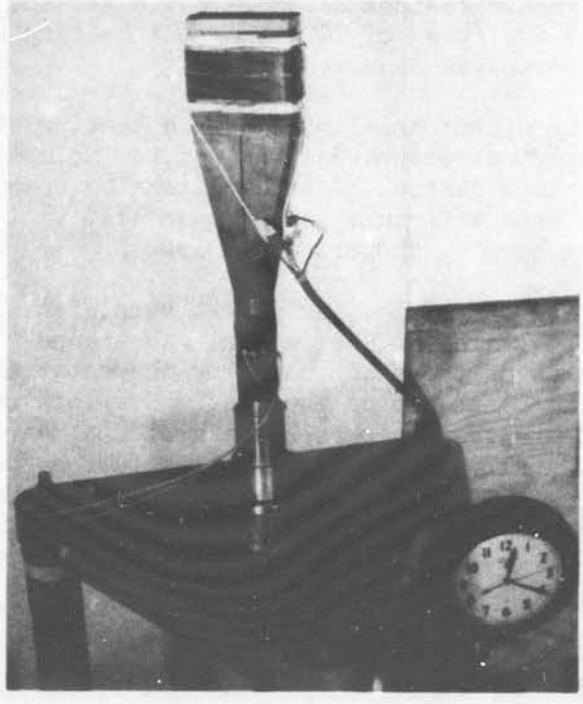

Figure 7. High-Frequency Vibratory System Mounted on Upper Main Plate.

rating of approximately five times that of the initial bearings. The bronze thrust washers were removed, and needle-bearing thrust washers were installed. With these changes, the low-frequency system operated satisfactorily.

HIGH-FREQUENCY SYSTEM

The high-frequency system (Figure 7) consisted of a magnetostrictive nickel-stack transducer-coupling system operating at a nominal frequency of 15,000 cycles per second. The assembly was attached to the upper main plate through a force-insensitive mount (described in Appendix III), which insured frequency stability under the applied loads and negligible loss of high-frequency energy to the support system.

The transducer was driven by the 600-watt electron-tube frequency converter as shown in Figure 4.

SPECIMEN MOUNTING

As previously noted, mounting the specimens was critical for effective energy transmission from the high-frequency system, because the clamped end of the specimen must excursion as an integral part of the clamping jaw and not exhibit the slightest degree of independent motion. The amplitude of high-frequency vibration was small, within the range of 0.0004-0.004 inch, and even microscopic differential motion would be unacceptable. Meticulous design of the mounting arrangement was therefore mandatory.

The grip ends of the systems were designed to allow interchangeability of specimens and at the same time to insure the necessary rigid connection. As shown in Figure 8, precision keyhole slots were provided in the ends of the specimen holders; these rectangular slots terminated in cylindrical holes, which were carefully reamed. The doubler-reinforced ends of the specimens were inserted in the slots, which had chamfered grip faces, and were secured with clamping bolts to prevent spreading of the jaws. Cylindrical pins were then press-fitted into the cylindrical holes to establish compressive loading and uniform contact between the ends of the specimen and the clamping jaws. A mounted specimen is shown in Figure 9.

This arrangement met the requirements for transmission of high-frequency vibratory energy.

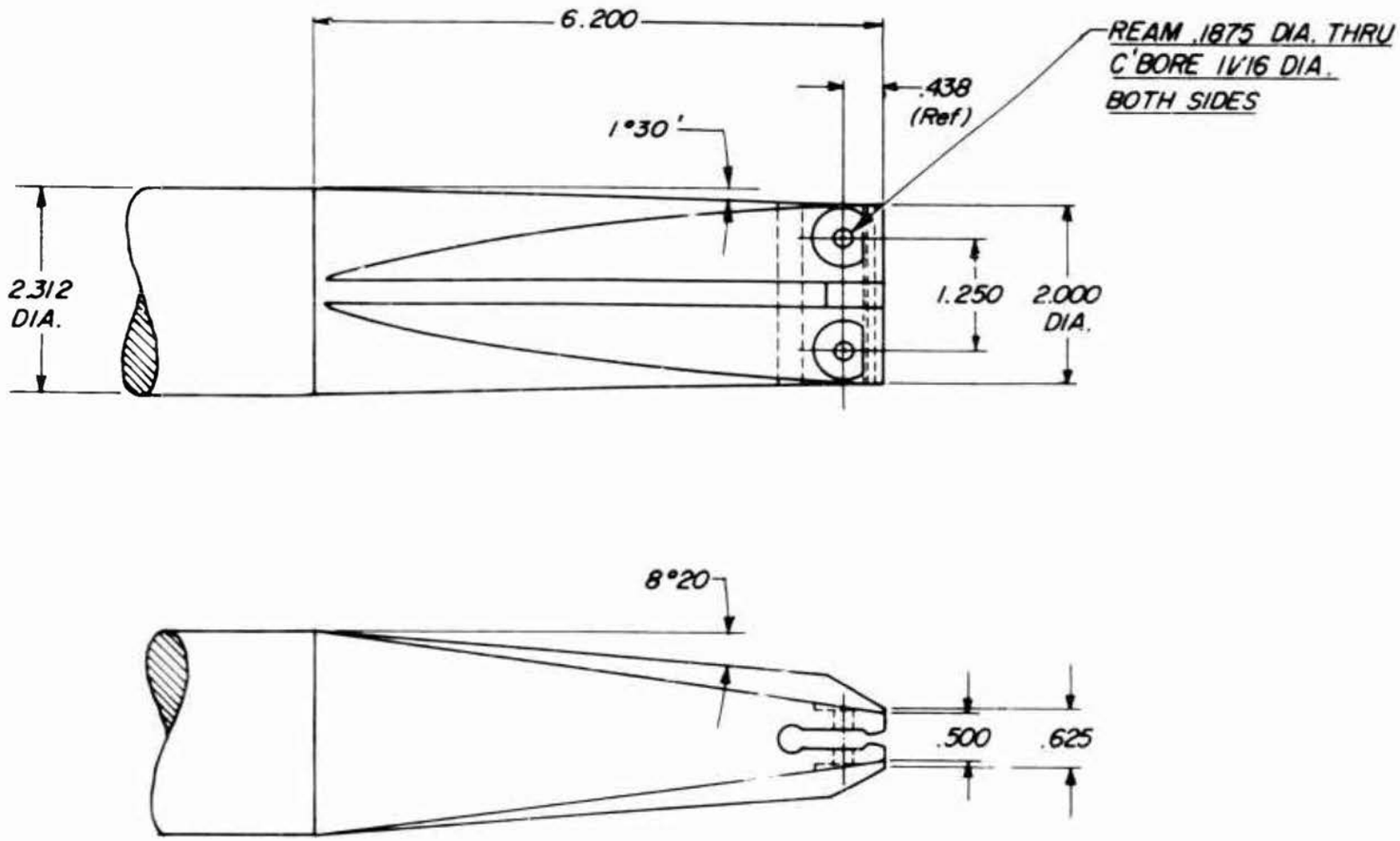

Figure 8. Design of Specimen-Holding Jaws.

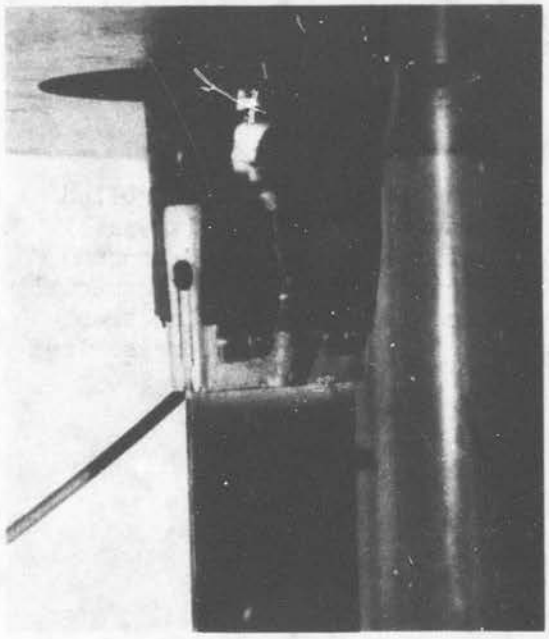

A. Upper Jaw Mounting

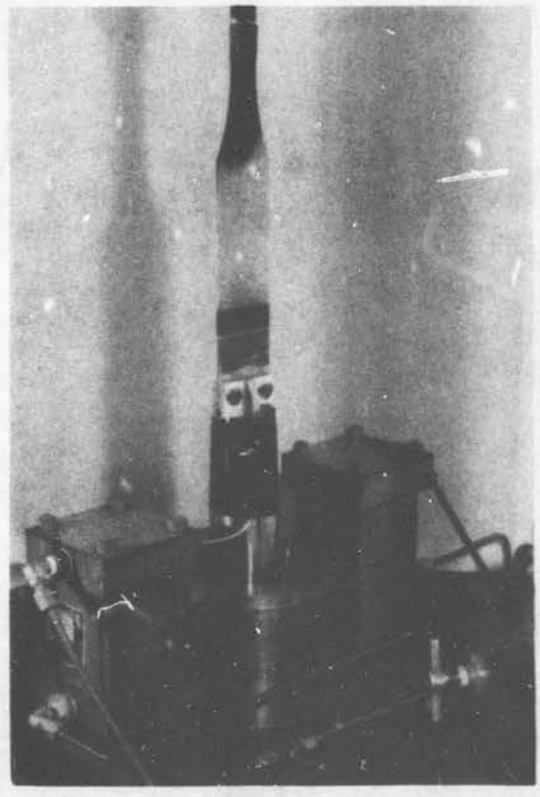

B. Lower Jaw Mounting.

Figure 9. Specimens Mounted in Clamping Jaws.

TEMPERATURE AND ATMOSPHERE CONTROL

The design of this machine permits specimen evaluation in controlled temperature and/or controlled atmosphere environments. A clam-shell type resistance heater or refrigeration coils can be mounted around the specimen to achieve the desired temperature and to house a special atmosphere. The specimen can readily be enclosed in a tubular transparent container, which could be purged of air and lightly pressurized with any desired gas.

INSTRUMENTATION AND DETERMINATION OF VARIABLES

Instrumentation was provided on the fatigue test equipment for measuring the variables of applied static load, static and low-frequency stress in the specimen, high-frequency electrical power input to the high-frequency system, high-frequency displacement amplitude of the specimen, specimen temperature, and number of cycles to failure.

STATIC LOAD

Static load was determined from the nitrogen pressure gage reading multiplied by the area over which the pressure was applied (piston area in the cylinders of 16.58 square inches) plus the weight of the low-frequency loading assembly. The pressure gages were calibrated with a tensiometer. The load was recorded on a strip-chart device which was calibrated against a standard strain gage previously calibrated on a universal tensile testing machine.

STATIC AND LOW-FREQUENCY STRESSES

The static stress in the specimen was readily determined by dividing the static load as obtained above by the cross-sectional area of the specimen in the center of the test section. This cross-sectional area was determined by direct measurement of each specimen.

For determination of the low-frequency stresses, a wire strain gage was bonded to each specimen, with its output being fed to the same channel of the strip-chart recorder that recorded the static load. At the outset of each test, the static load indicated on the strip-chart record was calibrated (by chart lines) against the calculated static stress. When low-frequency cyclic loading was then superimposed on the static loading, this calibration was used to determine the magnitude of the cyclic stress as indicated by the sinusoidal pen deflections on the chart. The strain gages used did not respond to ultrasonic frequencies, so that superimposed high-frequency vibration was not reflected on the chart readings.

The strip-chart record also provides a means for determining dynamic creep of the specimen during test. The creep is represented by the displacement of the centerline of the oscillatory force recording line from the static force line.

The static and low-frequency strains are derived from the recorded stress values, using the values of Young's modulus given in Table I.

HIGH-FREQUENCY POWER

High-frequency power input to the transducer of the high-frequency system was determined from a VAW meter installed in the line between the frequency converter and the transducer. The output from this VAW meter was connected to one channel of the strip-chart recorder to indicate any deviation in the prwer level.

HIGH-FREQUENCY DISPLACEMENT AMPLITUDE

Determination of the high-frequency cyclic stress at the center of the specimen was considered. Measurement of the stress per se in this locale is not amenable to measurement with strain gages, which are too low in frequency response. Optical methods for measuring local displacement are used extensively in our laboratory, but this specimen necessarily involved a double observation, including determination of phase relationship between displacements at opposite ends of the specimen. The possibility of mounting sensing crystals and obtaining accelerations was considered and abandoned, because extensive experimentation under essentially similar conditions has shown conclusively that the retention of the crystals is difficult under high-frequency vibration.

Thus it was evident that the problem of ascertaining local cyclic elongations within the gage portion of the specimen was totally unfeasible within the financial limitations of the contract. It was therefore concluded that the only reliable measurements could be made at the jaws, and such measurements did not discriminate phase. The average of the upper and lower displacement measurements, which provided a relative indication (neglecting phase differences) of peak-to-peak displacements within the test specimen, was recorded for the tests described later.

Any high-frequency displacement value can be used to determine the high-frequency strain $\mathcal{E}$ in a specimen from the equation

$$\mathcal{E} = \frac{2\pi f}{c} \xi \qquad (1)$$

where f is the frequency in cycles per second.

c is the velocity of sound in the specimen material in centimeters per second.

ξ is the peak-to-peak displacement per unit length of the specimen.

For measurement of displacements at the end points, barium titanate crystal elements were installed just behind the upper and lower specimen clamping jaws. The voltage outputs from these elements were fed

through high band-pass filters into separate channels of a strip-chart recorder. The filters were provided to eliminate response of the crystals to low-frequency vibration, so that their output was not influenced by the other type of loading.

The output voltage of the crystals was calibrated by means of a fiber optics sensing unit. With this device, light is conducted to within a few thousandths of an inch of a vibrating surface by half of the fibers comprising the fiber optics bundle. The remaining half of the fibers conduct the reflected light to a solid-state photosensitive cell. The electrical signal from this cell is proportional to the probe-to-surface separation and provides an accurate measurement of the vibratory amplitude. The instrument had been calibrated for dynamic response by the manufacturer, and this calibration was confirmed by comparison with microscopic observation of displacements obtained with a 15-kc ultrasonic system.

Typical calibration curves of displacement as a function of crystal output, obtained on upper and lower clamping jaws, are presented in Figure 10.

No straightforward means was available for determining the high-frequency stress in the specimen. It could not be calculated from the strain and Young's modulus, since the modulus of a material changes under the influence of ultrasonic vibration, and available literature provides no precise information on the magnitude of the change. Theoretically it should be possible to derive an expression for high-frequency stress as a function of high-frequency strain and the vibratory energy dissipated in the specimen. However, rigorous derivation and verification of such an expression were beyond the scope of this program.

It should be noted that the specimen midpoint is, by design, a displacement node and a stress antinode, so that under true standing wave conditions, no displacement should be detectable at the midpoint. However, as the acoustic transmission departs from true standing-wave conditions, the midpoint will exhibit high-frequency displacement proportional to the fraction of total energy that is transmitted through the specimen. It thus appears that a useful method for determining high-frequency strain (and perhaps high-frequency energy transmission and high-frequency stress) may be developed from analysis of the relationships existing among displacements observed at the midpoint and at the two end points.

SPECIMEN TEMPERATURE

The temperatures achieved in the specimen during fatigue testing were determined by means of an infrared radiometer located adjacent to the test machine (see Figure 4) and directed to monitor a small target area near the center of the specimen. This area of the specimen was coated

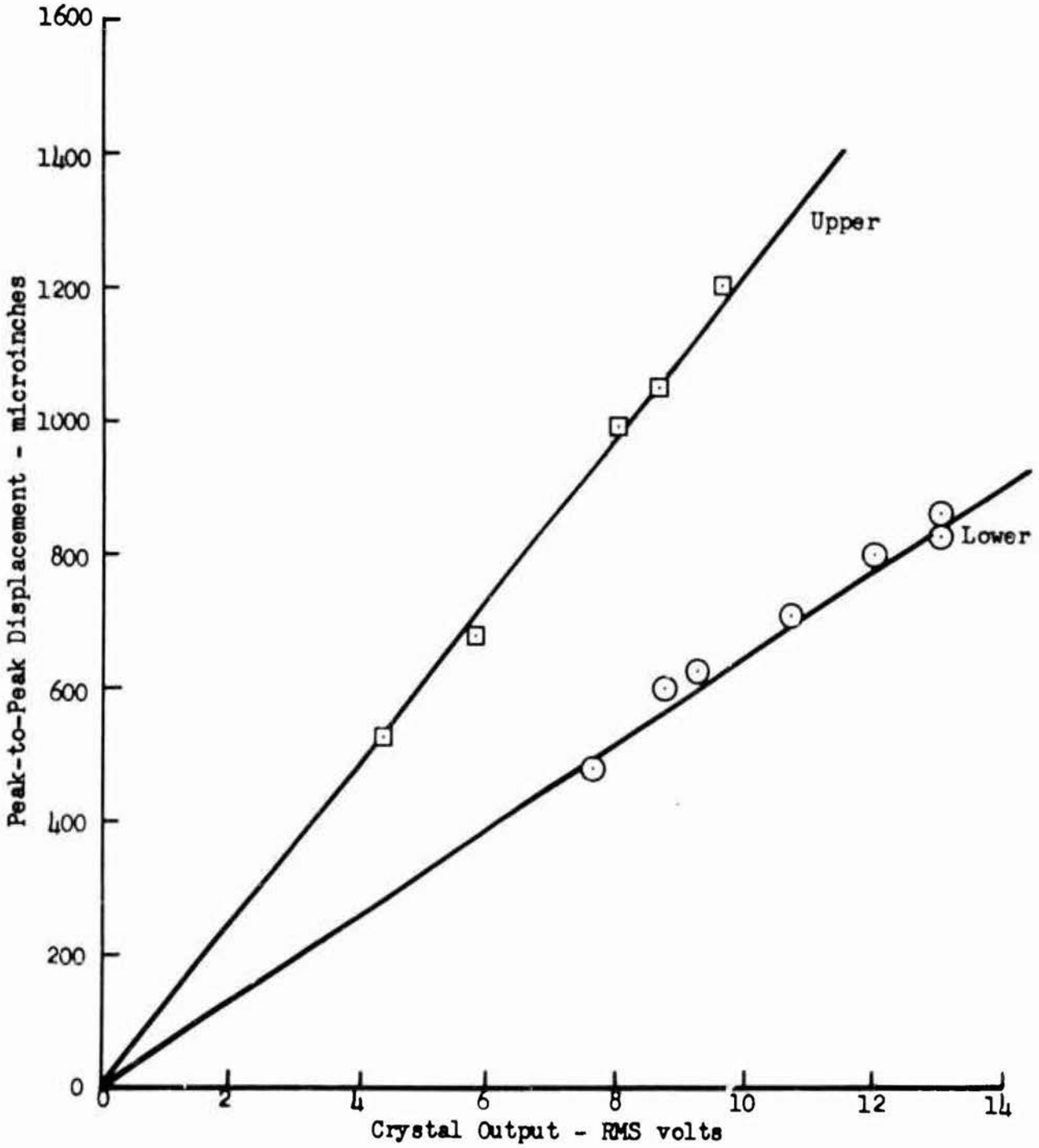

Figure 10. Typical Calibration Curves of Vibratory Displacement vs. Crystal Output at Upper and Lower Clamping Jaws.

with a flat black paint to provide the necessary high-emissivity surface. Simultaneous measurements made using the radiometer and a thermocouple indicated that such painted surfaces had an emissivity of 0.8, which is within the reported acceptable range of 0.79 to 0.84. The output of the radiometer was a voltage proportional to the temperature of the target surface. The unit was calibrated against data obtained from a Chromel-Alumel thermocouple embedded behind the view surface of an aluminum plate coated with the same black paint.

NUMBER OF CYCLES TO FAILURE

An electric timer with a sweep-second hand was used to measure the total time to failure. The timer was actuated at the instant of simultaneous application of low-frequency and high-frequency vibration to the specimen and was stopped at the instant of specimen failure. (An electronic timer could be incorporated into the test array to provide automatic starting and stopping.)

The number of cyclic loads per second for each test run was determined by means of a frequency counter. Measurements indicated that the transducer-coupling system operated at a frequency of 14,800 cycles per second with a tolerance of less than ± 100 cycles per second.

The low-frequency cyclic rate was determined by the running speed of the driving motor, which operated at constant speed regardless of load variation because of the relatively small loads on the higher capacity motor. The constancy of rotational speed and the number of low-frequency cycles to failure were confirmed from the sinusoidal variations on the strip-chart stress record.

DEMONSTRATION OF FEASIBILITY

The successful development of a compound loading apparatus (simultaneous high-frequency, low-frequency, and static loading) coupled with a sophisticated specimen configuration and necessary instrumentation brought the program to the point of feasibility demonstration.

This demonstration consisted first in subjecting various materials to the loading environment and then subjecting the various types of joints to the loading environment.

MATERIAL PERFORMANCE

The materials tested were AISI 4340 steel, 2014-T6 aluminum alloy, and 6Al-4V titanium alloy. Each material was fabricated into integral specimens in the configuration and to the dimensions described earlier (Figure 1 and Table I-E). Table II shows the loading input range used on these specimens.

Static and low-frequency forces were held essentially constant, while high-frequency forces were varied. This procedure permitted determination of the effect of the high-frequency vibration at several energy levels on the fatigue life of the specimens.

For the integral specimens, the selected static loads were equivalent to approximately three-fourths of the yield strength of each material. The magnitude of the superimposed low-frequency stress was then selected from Goodman diagrams, where available, to provide fatigue failure in the vicinity of 10^4 cycles (approximately 5 minutes at 2000 cycles per minute). Where Goodman diagrams were not available, the low-frequency stress values were selected by preliminary experimentation.

After measurements (made by dial caliper to ± .0001 inch) of the cross-sectional dimensions of the necked-down test section, the specimen was installed in the testing machine, and the weights on the rotating disks were adjusted to provide the desired low-frequency cyclic stress. The selected static load was applied first for strip-chart calibration, as shown on the typical chart record in Figure 11. This was followed by actuation of the low-frequency motor, the high-frequency power at the selected level, and the timer. On failure of the specimen, with automatic shut-off of the motor, the high-frequency power and the timer were manually terminated, and the time to failure was recorded.

Because of the lack of a straightforward method of determining high-frequency stress in the specimen, as discussed previously, the effects of the high-frequency vibration superimposed on the low-frequency and

Table II

LOADING CONDITIONS FOR INTEGRAL SPECIMENS

Material	Static Cylinder Pressure (psi)	Average* Static Tensile Stress (psi)	Low-Frequency			Average* Low-Frequency Cyclic Stress (psi)	High-Frequency	
			Frequency (cpm)	Moment Arm (in.)	Weight (grams)		Frequency (cps)	Power Range (watts)
Steel	300	79,200	1920	5.25	800	28,300	14,800	0 - 350
Aluminum	250	46,400	1920	5.25	632	54,000	14,800	0 - 350
Titanium	170	106,600	1920	5.25	632	63,900	14,800	0 - 350

* The average is based on data as presented in Table III.

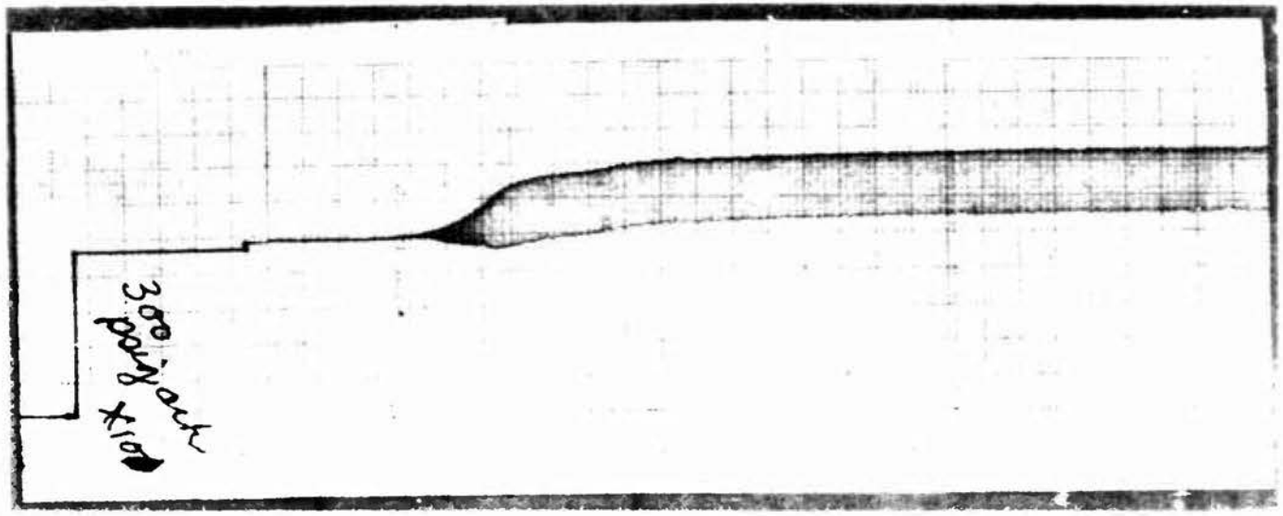

Figure 11. Representative Oscillograph of Strain Gage Output

Material: 4340 Steel.
Test Cross-Section Area: 0.0628 square inch.
Static Load: 4980 pounds.
Strip-Chart Speed: 10 mm/sec.
Dynamic Creep: Indicated by deviation of centerline of trace from horizontal.

static stresses were plotted in terms of total time to failure as a function of input power to the ultrasonic system. Table III summarizes the data obtained, including the actual static and low-frequency stresses (based on measured specimen cross-sectional areas), the recorded displacement amplitude of high-frequency excitation, and the total time to failure. Figure 12 provides plots of the failure time as a function of high-frequency power input.

Steel Specimens

The specimens of annealed 4340 steel were subjected to a nominal static stress of 80,000 psi and a superimposed low-frequency stress of ± 30,000 psi at a frequency of 1920 cycles per minute, which, according to an available Goodman diagram, should provide a specimen life within the range of 1×10^4 to 2×10^4 cycles. For the specimens tested without superimposed high-frequency loading (zero ultrasonic power), failure actually occurred at 1.4×10^4 cycles of low-frequency excitation. Thus the equipment and the material functioned as predicted.

As shown in Figure 12-A, high-frequency excitation shortened the life of the specimen, with the elapsed time to failure becoming shorter as the ultrasonic power was increased. At the maximum power level of 350 watts, the specimen failed in 78 seconds or after approximately 1.2×10^6 high-frequency cycles.

During these tests, substantial heating of the specimen occurred, as revealed in Figure 13. In the control specimen (zero ultrasonic power), the temperature rose slowly and reached a maximum of about 40°C during the 7 minutes 20 seconds of test. As the ultrasonic power was increased, the temperature rose increasingly rapidly and reached a maximum in the range of 60-70°C just before failure occurred. A typical fracture in the steel is shown as Specimen B in Figure 14.

Aluminum Alloy Specimens

The 2014-T6 aluminum alloy specimens were subjected to a nominal static stress of 47,000 psi and a superimposed low-frequency stress of ± 60,000 psi at 1920 cycles per minute, which, according to the Goodman diagram, should provide a life of about 10^4 cycles. In the control test (zero ultrasonic power), specimen failure occurred after 470 seconds, at 1.5×10^4 cycles of low-frequency excitation.

The effect of high-frequency stressing is plotted in Figure 12-B, which shows the decrease in specimen life as a function of the high-frequency power level. The data for these tests may be distorted by the fact that the specimens exposed to the highest ultrasonic power levels failed, not

Table III

TEST DATA FOR INTEGRAL SPECIMENS

Material	Young's Modulus (10^6 psi)	Test Area (in.^{2})	Static		Low-Frequency		High-Frequency		Elapsed Time to Failure (sec)	Cycles-to-Failure of Low-Frequency Excitation
			Stress (psi)	Peak Strain (μin./in.)	Stress (psi)	Peak Strain (μin./in.)	Power Input (watts)	Peak-to-Peak Displacement (μin.)		
4340 Steel	30.8	0.0630	78,000	2530	32,200	525	0	-	440	14,080
		0.0628	79,500	2580	30,800	500	150	54	435	13,920
		0.0638	78,000	2530	29,180	470	200	55	360	11,520
		0.0615	81,000	2630	29,200	475	280	118	243	7,776
		0.0625	79,500	2580	20,000	325	350	90	78	2,496
2014-T6 Aluminum Alloy	10.2	0.0600	46,000	4500	66,000	3230	0	-	470	15,040
		0.0610	46,300	4530	42,400	2215	55	180	465	14,880
		0.0592	46,200	4520	67,700	3315	110	318	120*	3,840
		0.0596	47,400	4620	51,100	2500	175	600	105*	3,360
		0.0612	46,200	4520	43,000	2110	350	673	23*	736
6Al-4V Titanium Alloy	16.6	0.0392	105,800	6400	58,800	1785	0	-	840	26,880
		0.0373	106,800	6470	76,200	2310	100	258	210	6,720
		0.0395	106,000	6430	42,400	1270	150	461	750	24,000
		0.0373	106,800	6470	70,000	2115	175	400	1290	41,280
		0.0385	107,500	6520	71,900	2160	350	498	750	24,000

* Failed at doubler.

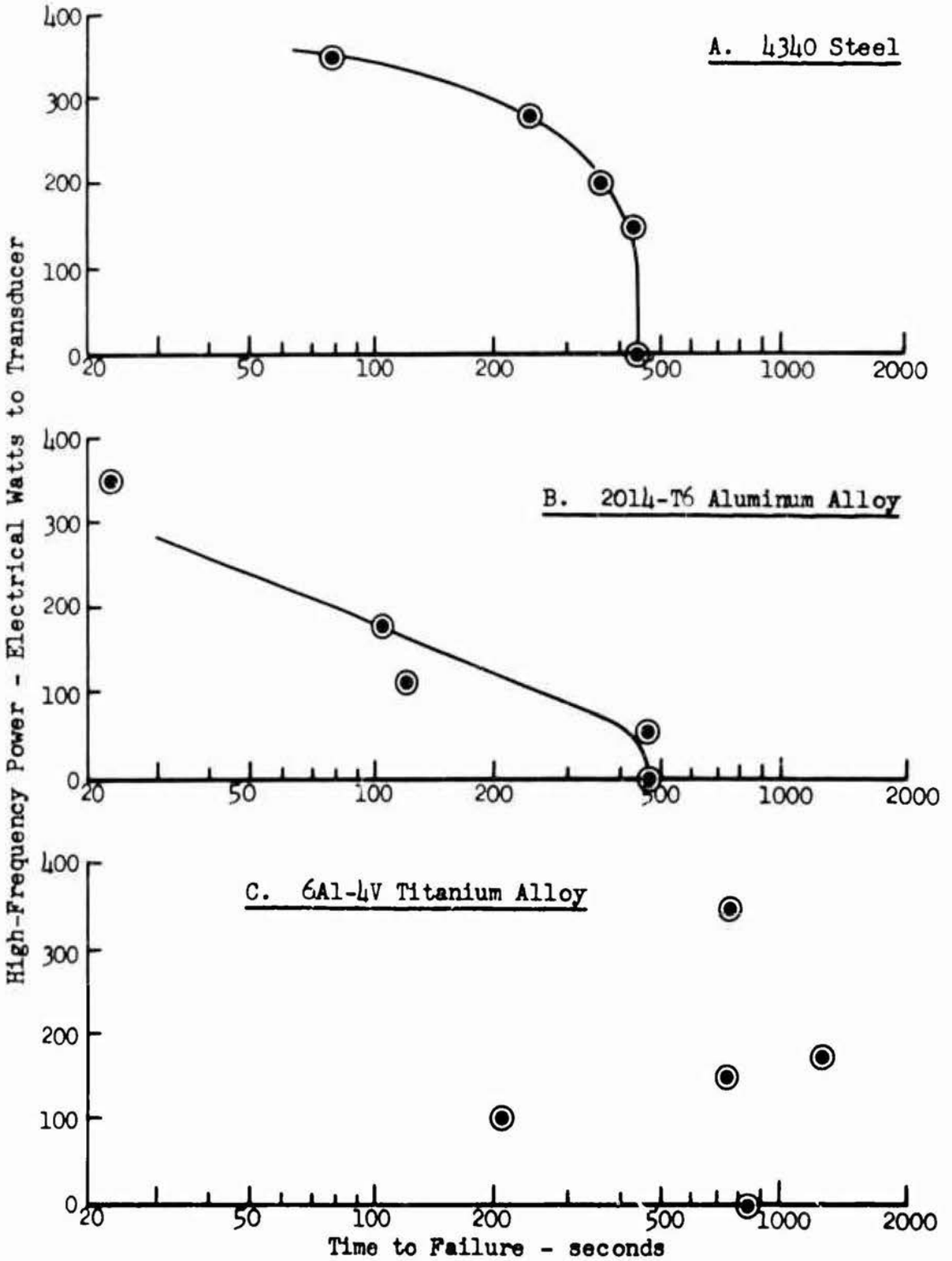

Figure 12. Effect of High-Frequency Vibration on Fatigue Life of Integral Specimens.

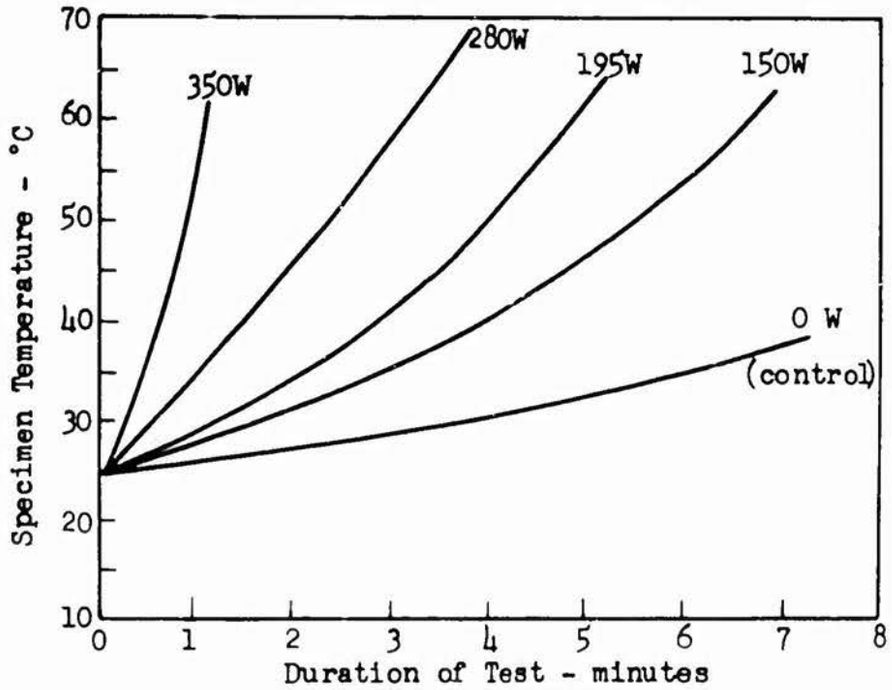

A. Temperature Rise as a Function of Applied Ultrasonic Power.

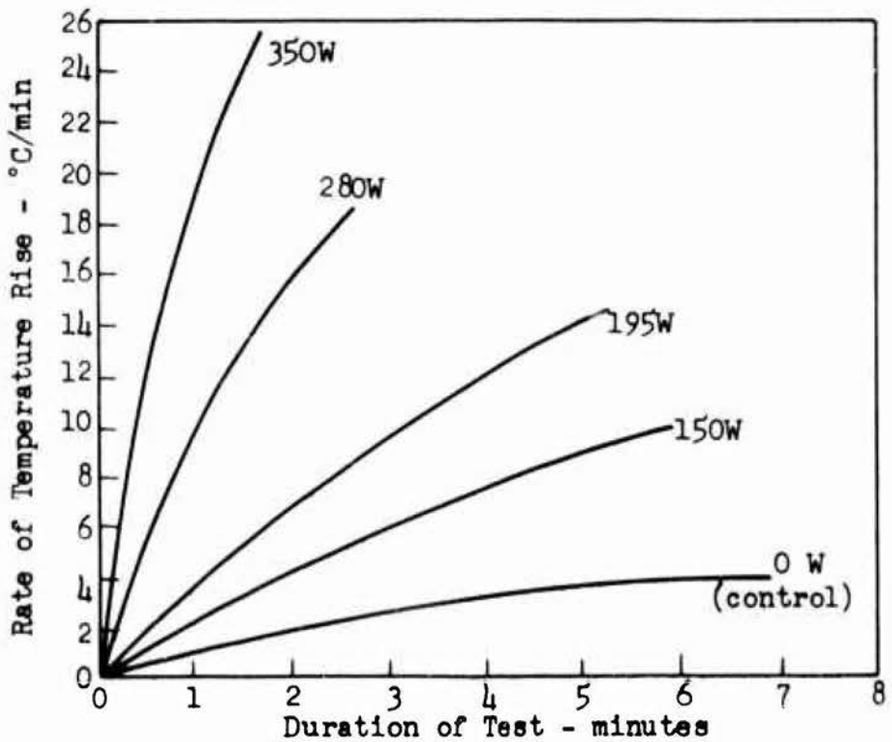

B. Rate of Temperature Rise as a Function of Applied Ultrasonic Power.

Figure 13. Effect of High-Frequency Stressing on Specimen Temperature and Rate of Temperature Rise for 4340 Steel.

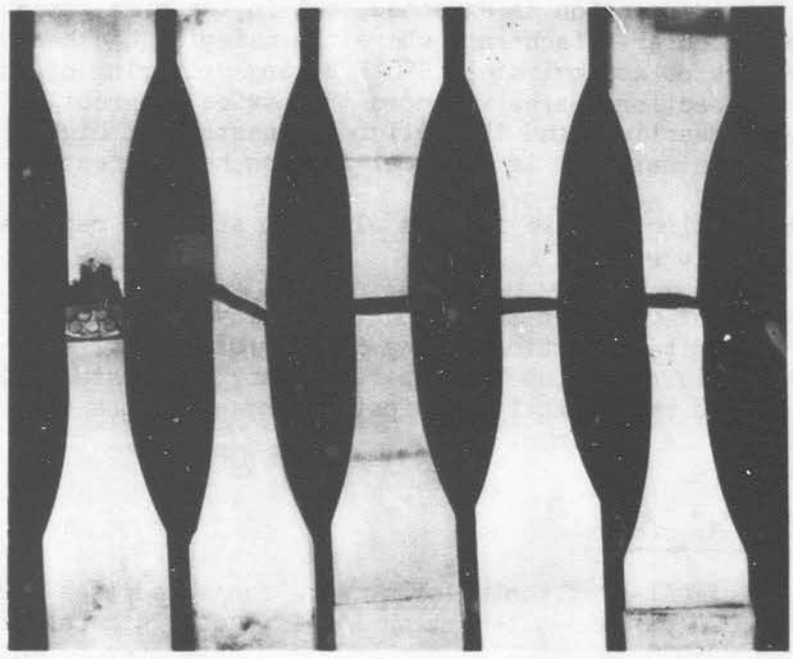

A B C D E

Figure 14. Typical Fatigue Failures of Specimens Under Combined Static, Low-Frequency, and High-Frequency Loading.

A. Riveted Steel Specimen.

B. Integral Steel Specimen.

C. Integral Titanium Alloy Specimen.

D. Integral Aluminum Alloy Specimen.

E. Butt-Welded Steel Specimen.

at the specimen midsection as expected, but in the area immediately adjacent to the doubler attachment, where the material had been exposed to a temperature of approximately 550°F during soldering of the doublers. Here the cross-sectional area was more than twice as great as that in the specimen midsection, and the failure suggests that high-frequency stressing of this material is critical in such heat-affected zones.

A typical midsection failure in this aluminum alloy is represented by Specimen D in Figure 14.

Temperature measurements in these aluminum alloy specimens failed to reveal any significant heating during fatigue stressing, even at the highest ultrasonic power level. Apparently any temperature rise that may have occurred was promptly dissipated because of the high thermal conductivity of the aluminum.

Titanium Alloy Specimens

The specimens of 6Al-4V titanium alloy were subjected to a nominal static stress of 106,000 psi and alternating low-frequency stresses ranging from ± 42,000 to ± 76,000 psi at 1920 cycles per minute over a nominal cross-sectional area of 0.38 square inch. No Goodman diagram was available for this material.

The application of high-frequency alternating stresses over the power range of 0 to 350 watts did not generate any definable relationship to specimen life, as evidenced by the scatter of points on the plot of Figure 12-C. Moreover, no perceptible change in temperature was observed under any of the combined loading conditions. Thus, in contrast to the steel and aluminum alloy, the titanium alloy appeared to be relatively impervious to high-frequency vibratory effects within the range of high-frequency power applied. Doubtless, higher power levels will produce a clearly evident effect.

A possible explanation may be found in the acoustic hysteresis of these materials. In previous investigations in our laboratory (reference 6), the comparative hysteresis properties of several materials had been determined by acoustic calorimetric techniques. The results of that work, reproduced in Figure 15, indicate the power loss as a function of high-frequency strain to be substantially greater for steel than for titanium alloy. The peak strains achieved during the fatigue test were functions of the combined static, low-frequency, and high-frequency loading, and it is to be expected that those strains would involve power loss values for steel greatly exceeding those for the titanium. This difference in power dissipation may partially explain the fatigue behavior of the titanium alloy under the superimposed high-frequency stresses.

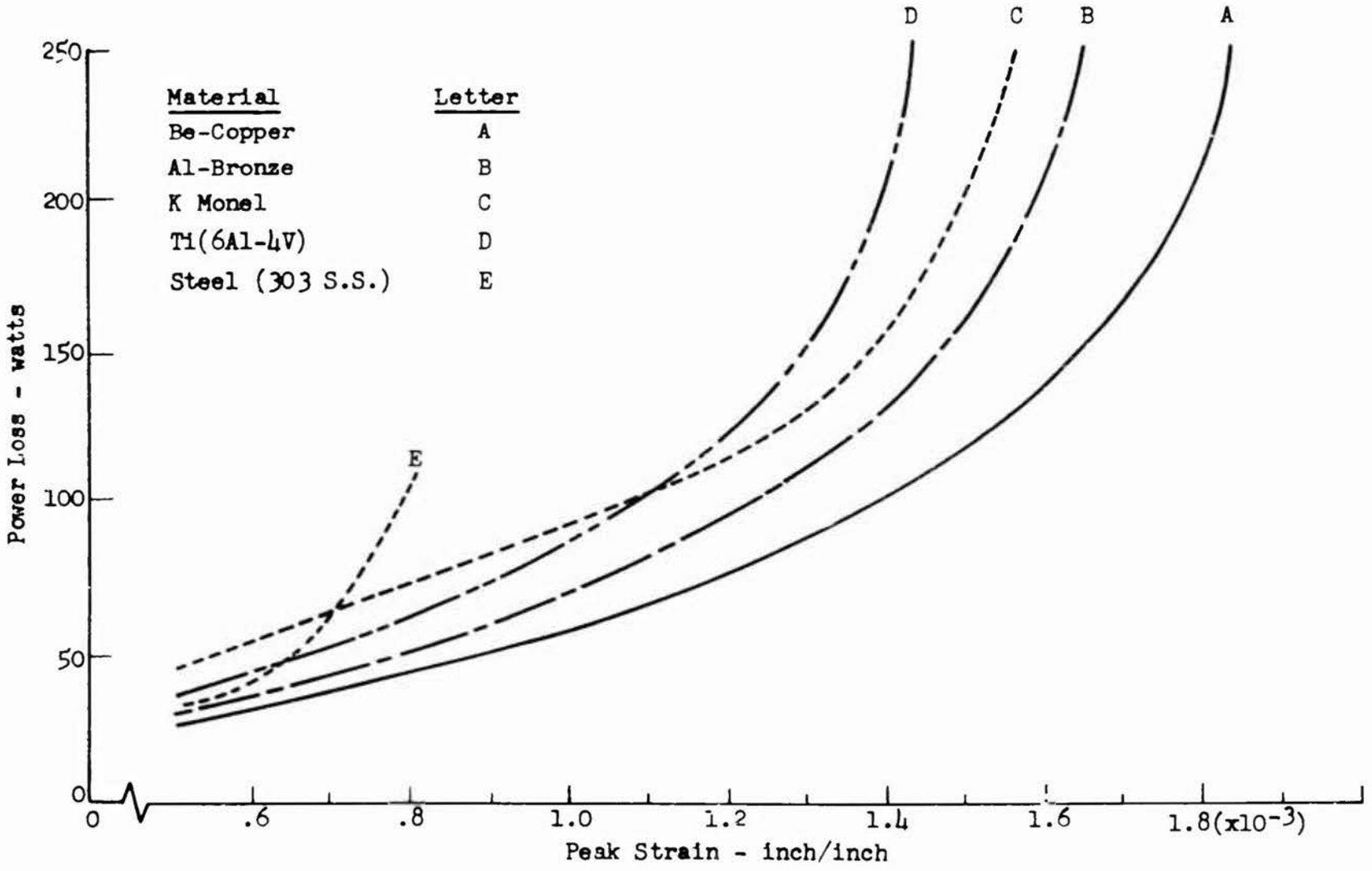

Figure 15. Power Loss and Strain Characteristics of Candidate Coupler Materials at 15 Kilocycles per Second.

More comprehensive testing over a broader range of conditions, including substantially higher ultrasonic power levels, would be necessary to confirm the observed trend.

JOINT PERFORMANCE

The second portion of the demonstration was concerned with subjecting various joint specimens of 4340 steel to the combined loading apparatus environment. Table IV shows the loading input range used on the various joints.

Table IV

LOADING CONDITIONS FOR JOINT SPECIMENS OF 4340 STEEL

Type of Joint	Static Cylinder Pressure (psi)	Low-Frequency			High-Frequency	
		Frequency (cpm)	Moment Arm (in.)	Weight (grams)	Frequency (cps)	Power Range (watts)
Welded	260	1920	5.25	1659	14,800	98 - 350
Riveted	150	1920	5.25	632	14,800	0 - 350
Adhesive-Bonded	66.6	1920	5.25	39	14,800	0 - 350
Brazed	200	1920	5.25	1380	14,800	0 - 350

Except for the butt-welded joints, all of the joints were of the single-overlap type, in which axial loading involved an eccentricity which undoubtedly influenced the indicated fatigue life. Furthermore, with such an overlap joint, where failure occurred in shear in the joint, it was not possible to determine the cross-sectional area over which the forces acted. Consequently, no accurate determination could be made of the static or low-frequency stresses acting on the joints or the strains induced in the specimens. In these cases the loads on the specimens were recorded in pounds.

The fatigue test data for these joints are summarized in Table V, and the total times to failure are plotted as a function of high-frequency power input in Figure 16.

Table V

TEST DATA FOR JOINT SPECIMENS OF 4340 STEEL

Type of Joint	Test Area ($in.^2$)	Static Stress/ Load(a)	Low-Frequency Stress/ Load(a)	High-Frequency Power Input (watts)	High-Frequency Peak-to-Peak Displacement (μin.)	Elapsed Time to Failure (sec)
Fusion	0.0603	71,700 psi	63,600 psi	98	348	17.5
Welded	0.0603	71,700	50,300	175	445	12
	0.0624	69,200	60,500	350	(b)	9
Riveted	-	2490 lb	1780 lb	0	-	7
	-	2490	2010	175	(b)	10
	-	2490	1832	350	470	5
Adhesive-Bonded	-	1110 lb	1600 lb	0	-	68
	-	1110	1375	200	475	48
	-	1110	1560	350	(b)	4
Brazed	-	3320 lb	4050 lb	0	-	45
	-	4150	2930	150	375(c)	13
	-	4150	2760	350	545(c)	9

(a) Stress in psi for welded butt joint specimens; load in pounds for lapped joint specimens.

(b) Indeterminate.

(c) Displacement of upper jaw only.

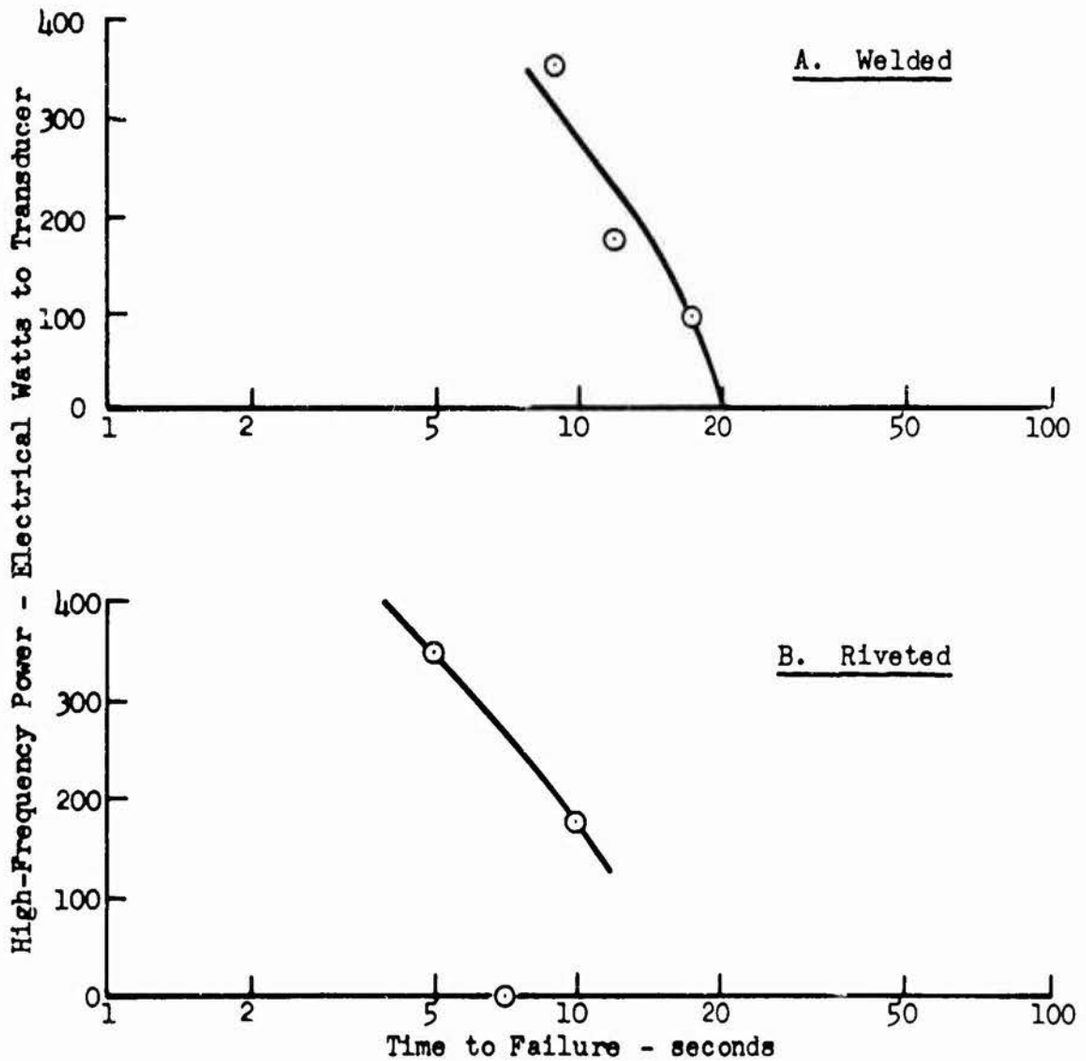

Figure 16. Effect of High-Frequency Vibration on Fatigue Life of Joint Specimens of 4340 Steel

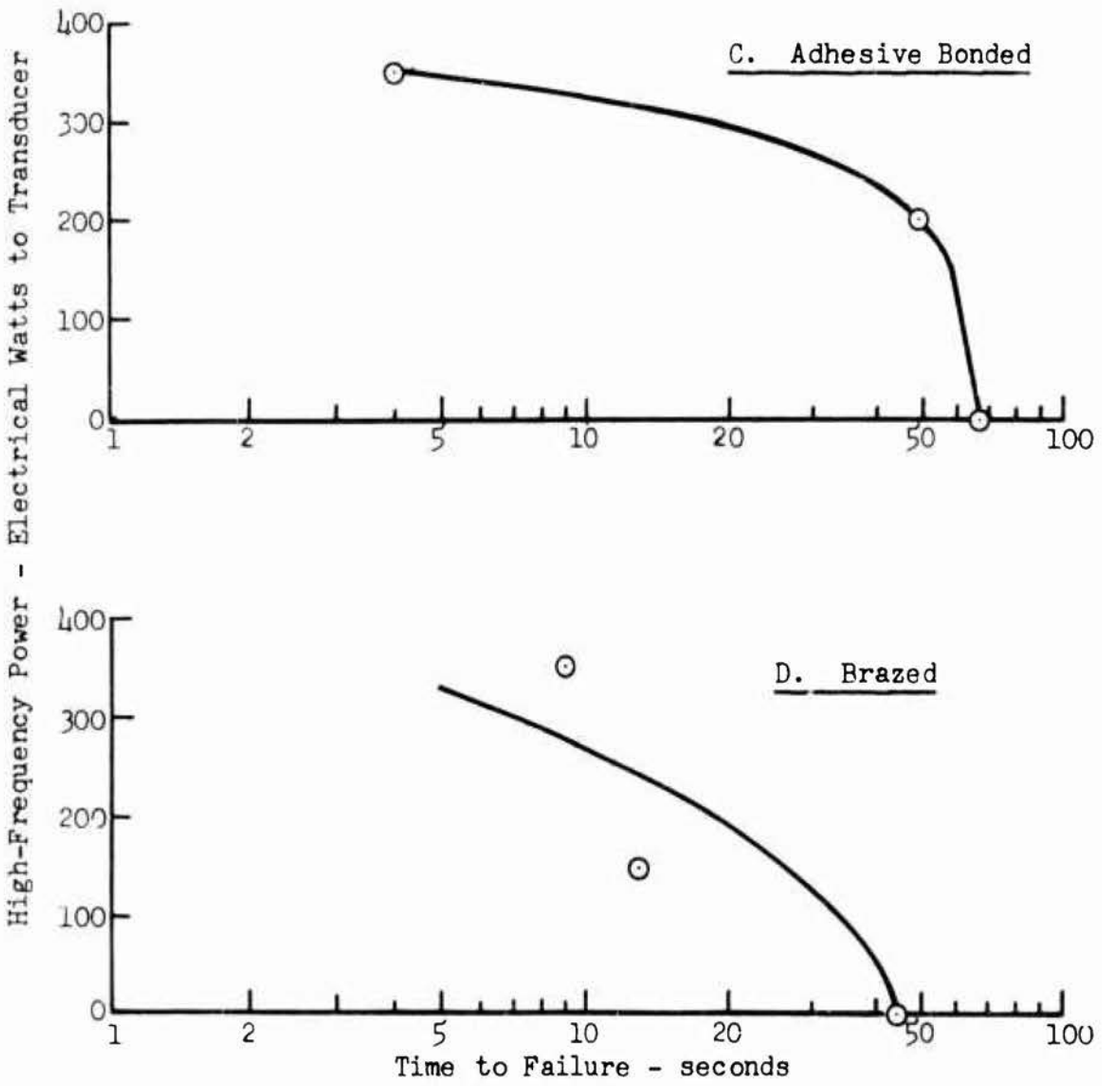

Figure 16 (concluded). Effect of High-Frequency Vibration on Fatigue Life of Joint Specimens of 4340 Steel

Welded Specimens

Under the conditions used, the butt-welded specimens were subjected to static stresses of 70,000 psi and low-frequency alternating stresses of ± 50,000 psi at 1920 cycles per minute over a nominal cross-sectional area of 0.06 square inch. Applied high-frequency power ranged from 98 to 350 watts.

As shown in Figure 16-A, these specimens demonstrated a decrease in fatigue life with increasing ultrasonic power. No perceptible change in specimen temperature was observed during any of the tests. In all cases, failure occurred just above the weld area, along the boundaries of the heat-affected zone resulting from the fusion-welding temperatures. A typical failure is shown as Specimen E in Figure 14.

Riveted Specimens

These specimens were subjected to a constant static load of 2490 pounds and an alternating load of approximately ± 2000 pounds at 1920 cycles per minute. High-frequency alternating stress was varied over a range represented by input powers ranging from 0 to 350 watts.

The resulting data (Figure 16-B) from these limited tests do not show the well-defined trend observed with the other types of joints. The specimen stressed at low high-frequency power (150 watts) showed a longer fatigue life than the specimen stressed at zero ultrasonic power. More extensive testing would be necessary to establish whether there is actually an ultrasonic effect.

Specimen failure was characterized by tearout of the parent metal rather than by rivet shear, as shown by Specimen A in Figure 14. This apparently resulted from bending of the ends of the specimen half-sections due to the eccentricity of loading created by the lap geometry. This eccentricity caused the rivet heads to bear against the parent metal, producing areas of stress concentration which accelerated failure.

Adhesive-Bonded Specimens

These lap-type specimens were subjected to a constant static load of 1110 pounds and alternating loads within the range of ± 1300 to ± 1600 pounds at 1920 cycles per minute. High-frequency electrical power was varied from 0 to 350 watts.

Figure 16-C shows a decrease in specimen life as the high-frequency power was increased. The maximum power of 350 watts produced failure in 4 seconds (7.1×10^4 cycles of high-frequency excitation), whereas the non-ultrasonically stressed specimen required 68 seconds to failure (13×10^4 low-frequency cycles). In every case, failure was in shear through the epoxy bond.

Brazed Specimens

The lap-type brazed specimens were subjected to constant static loads of 3320 and 4150 pounds, to low-frequency alternating loads within the range of ± 2700 to ± 4000 pounds, and to high-frequency power input levels ranging from 0 to 350 watts.

The results of these tests (Figure 14-D) likewise showed decreasing specimen life with increasing ultrasonic power. Failure invariably occurred in shear through the braze bond.

EVALUATION OF EQUIPMENT AND CONCLUSIONS

The contractor succeeded in developing a compound loading apparatus that provides for:

1. Interchangeability of test specimens.

2. Adjustable controlled loading of the specimens simultaneously with the following:

   a. High-frequency fatigue loading at a nominal frequency of 15,000 cycles per second.

   b. Superimposed normal fatigue loading at a frequency of 2000 cycles per minute.

   c. Superimposed steady-state static loading.

The equipment performed satisfactorily in tests of varying time duration up to a maximum of nearly 1/2 hour. The high-frequency vibratory energy transmission system incorporated in the apparatus excited the specimen test section to a maximum vibratory amplitude, at 350 watts electrical power input to the transducer, of 0.0008 inch. Thus, good impedance matching was obtained through the transducer-coupling system to the holding jaws and into the test specimen.

The feasibility of the apparatus as a fatigue test instrument was clearly shown, as specimen life in several instances was significantly altered by varying the input level of high-frequency vibration. Units that did not experience the alteration in life either possessed sufficiently different internal characteristics or experienced loading variation due to clamping arrangements.

In addition, there is evidence that the apparatus will allow comparative evaluation of various materials as well as various structures in their response to compound fatigue loading environments. This would allow meaningful analog test program analysis of proposed configurations. Evaluation of a complete joint or structure response could be accomplished in subscale units.

Thus, the equipment is adequately suited to laboratory testing of materials and various joint designs for knowledge of materials behavior under conditions encountered in rocket-propelled vehicles. The data obtained on the several materials and joints used in this program conclusively affirm that specimen life may be significantly reduced by the superposition of high-frequency vibration on static and low-frequency vibration for many specimen types. The data also indicate that for some

materials and specimen types (e.g., integral titanium with mechanically connected end fittings), the specimen requires a substantially higher level of high-frequency vibratory power.

It is thus apparent that further use of the equipment developed may include determination of those materials and joint types possessing the best life (and possibly endurance) characteristics under the compound vibration conditions existing in rocket-propelled flight. This may include determination of S-N type curves, assuming that a rigorous method is established for determination of high-frequency stress. In such a case, the ordinate of the curve would be the total stress:

$$S_t = S_{st} + S_{lf} + S_{hf} , \qquad (2)$$

where S_{st} is the static stress,
S_{lf} is the low-frequency stress,
S_{hf} is the high-frequency stress.

An alternate approach would be the empirical development of a Goodman-type diagram of essentially three dimensions, on which a third orthogonal axis would be added to include the effect of high-frequency stress as measured by input power to the high-frequency excitation system.

Preliminary calculations of energy density levels developed in the specimen indicate strongly that the high-frequency vibration provides a greater energy input than the low-frequency vibration. The possibility of the energy density level's being a controlling parameter can be easily determined on the apparatus.

RECOMMENDATIONS

In view of the successful demonstration of the capabilities of the complex fatigue loading apparatus, it is recommended:

1. That this investigation be extended to encompass large numbers of specimens of selected materials, in order to establish the critical parameters controlling the performance of the materials when subjected to complex fatigue loading. The resulting data should be correlated with available Goodman diagrams and low-frequency fatigue data.

2. That similar effort be expended in evaluating joint design, utilizing subscale analog testing and covering a wide range of structural configurations.

3. That the work be extended to include evaluation of materials and joints at various temperatures and under various atmospheric conditions.

4. That the instrumentation be further developed to allow precise determination of high-frequency stress and possible interactions of loading input.

BIBLIOGRAPHY

1. Bianchi, R. A., R. T. Bradshaw, J. H. Farrell, and F. E. Reed, "Survey and Evaluation of Sonic Fatigue Testing Facilities", Technical Report No. ASD-TR-61-185, CONESCO Consultants in Engineering Science, Arlington, Massachusetts, Contract AF 33(616)-7003, March 1962.

2. Elmore, W. C. (Aeroprojects Incorporated), "Support for Vibratory Devices", U. S. Patent Number 2,891,180, June 16, 1959.

3. Fox, A., "A Comparison of Ultrasonic and Conventional Axial Fatigue Tests on Aluminum Alloy Rod", Materials Research and Standards, February 1965, pp. 60-63.

4. Gaines, N., "A Magnetostriction Oscillator Producing Intense Audible Sound and Some Effects Obtained", Physics, Volume 3, 1932, pp. 209-229.

5. Goetze, D., "Ultrasonic Machining of Tungsten Carbide", Transactions of the IRE, Volume PGUE-4, August 1956, pp. 19-22.

6. Jones, J. B., N. Maropis, et al., "Development of Ultrasonic Welding Equipment for Refractory Metals", Report ASD TR 7-888, Volume 2, Aeroprojects Incorporated, West Chester, Pennsylvania, Air Force Contract AF 33(600)-43026, December 1961, Appendix IV, "Coupler Material Studies".

7. Mason, W. P., Piezoelectric Crystals and Their Application to Ultrasonics, D. Van Nostrand Company, Inc., New York, New York, 1950, pp. 162-164.

8. "Metallic Materials and Elements for Flight Vehicle Structure", MIL-HDBK-5, Department of Defense, Washington, D. C., August 1962, Chapter 8.

9. Trapp, W. J., and B. J. Lazan, "Role of Structural Damping in Acoustical Fatigue", WADC Technical Report 59-304, University of Minnesota and Wright Air Development Division, Project Number 7360, January 1960.

APPENDIX I

CHRONOLOGICAL LITERATURE REVIEW ON HIGH-FREQUENCY FATIGUE TESTING

1925

1. Jenkin, C. F., "High-Frequency Fatigue Tests", Proceedings of the Royal Society, London, Volume 109A, 1925, pp. 119-143.

Wire specimens of copper, Armco iron, and mild steel were vibrated by means of alternating electrical power. Each specimen was supported at the nodes in brass trunnions and placed between the poles of an electromagnet, which produced a nearly uniform horizontal field normal to the test piece. Alternating current flowing along the specimen caused it to vibrate in the magnetic field, at the natural frequency of the test piece. The tests were run until the specimen fractured or 10^7 cycles had been completed. The low-frequency tests at 50 cps lasted 55 hours or less. Those at 500 cps lasted for 5-1/2 hours or less, and the 1000-cps tests required 2-3/4 hours or less. The highest frequency (2000 cps) required no more than 83 minutes. The Armco iron and steel samples failed suddenly, but the copper samples failed more gradually. The first sign of failure was a reduction in vibratory amplitude.

To test these metals at higher frequencies, the equipment was altered to produce torsional vibration. None of the copper rods or tubes were fractured, even during a test which continued to 60 million cycles at a frequency of 4000 cps.

1929

2. Jenkin, C. F., and G. D. Lehmann, "High Frequency Fatigue", Proceedings of the Royal Society, London, Volume 125A, 1929, pp. 83-119.

The effect of the frequency of alternating stress on the fatigue limits of various metals was investigated, with air pressure supplying the vibratory power. The specimens were vibrated by two blowers, each of which consisted of an adjustable resonating chamber into which air was admitted by a throttle in the back. The front was closed by one face of the specimen, which was arranged so that its vibrations to and fro alternately released the air pressure or allowed it to mount up in the chamber.

Tests were made on copper, steel, aluminum, and Armco iron bars at frequencies ranging from 50 to 20,000 cps. Strains were calculated on the assumption that the specimens vibrated freely and that the only measurement required was the amplitude of vibration at the center of the bar.

Increases in fatigue limit up to 60 percent were recorded, but the observed fatigue limit did not increase indefinitely. When a maximum value was reached in some tests, the limit at the highest frequencies actually fell.

1932

3. Gaines, N., "A Magnetostriction Oscillator Producing Intense Audible Sound and Some Effects Obtained", Physics, Volume 3, 1932, pp. 209-229.

In using a nickel-tube magnetostrictive transducer operating at 8900 cps for studying various ultrasonic effects, Gaines found that the nickel tubes were all eventually broken near the middle, due to fatigue of the metal. Measurements indicated that the amplitude of tube vibration was 0.01 mm in water and 0.03 mm in air, the latter corresponding to a stress of 11,500 psi. Breakage occurred within 15 to 90 minutes (i.e., within 8- to 48-million cycles). The author suggested this device as a means for quickly fatiguing magnetostrictive materials in evaluation of their physical properties.

1950

4. Mason, W. P., Piezoelectric Crystals and Their Application to Ultrasonics, D. Van Nostrand Company, Inc., New York, New York, 1950, pp. 162-164.

Mason described an apparatus useful for fatigue testing of metals, consisting of a piezoelectric crystal mosaic glued to an exponentially tapered coupler to which was screw-attached a metal specimen with a narrowed central section. With the total length of coupler and specimen equal to an integral number of half-wavelengths, no appreciable strain was developed at the glued joint, which was located at a vibratory antinode. With a diameter reduction from 3 inches at the crystal to 0.05 inch in the necked-down section of the specimen, located at a vibratory node, the strain was amplified by a factor of 40. Such a device was reported to permit investigation of the fatigue properties of metal at a high rate of strain and velocity.

1951

5. Drew, D. A., "Measuring Stresses in Aircraft Turbines", Engineering, December 14, 1951, pp. 761-763.

The cause of turbine bucket failures on aircraft gas turbines was investigated on the test-bed and in flight. The high-frequency investigations

were conducted in the laboratory on model cast aluminum buckets. A magnetostrictive nickel-stack transducer and an exponential steel coupler were used to deliver the ultrasonic energy to the test specimens at 13.2 kc. For maximum transfer of energy to the bucket, it was necessary to match the motional impedance of the load with that of the stack and coupler assembly. Wire-wound strain gages were attached to the buckets to measure the stresses. No results were presented.

1953

6. Neppiras, E. A., "Some Applications of High-Power Ultrasonics in the Metal Industries", Metal Treatment and Drop Forging, Volume 20, 1953, pp. 391-398.

Among other applications, the use of ultrasonics for accelerated fatigue testing is described. Preferably a magnetostrictive transducer is coupled through a step-up exponential mechanical transformer to a longitudinally resonant specimen, the joint being located at a displacement antinode. For frequencies above about 100 kc, crystal transducers were recommended. Such devices could also be used for accelerated life tests to determine metal behavior under periodic forces, such as hammer blows or frictional forces.

1956

7. Mason, W. P., "Internal Friction and Fatigue in Metals at Large Strain Amplitudes", Journal of the Acoustical Society of America, Volume 28, 1956, pp. 1207-1218.

Apparatus for producing high strains in metals consisted of a barium titanate cylinder, a half-wave exponential horn with diameter reduced from 3 inches to 0.25 inch, and a second half-wave exponential horn, screw-attached to the first and including the test specimen, with diameter reduced from 0.25 inch to 0.060 inch. This arrangement provided a step-up in strain by a ratio of 50:1. Further step-up to 250:1 was achieved by cutting a smaller radius in the horn. Measurements of the impressed voltage and a pickup voltage on the barium titanate made it possible to calibrate the device for determination of internal friction, change in elastic constant, and strain in the sample. Such measurements were made on lead and aluminum during stressing to fracture, and the results were analyzed in terms of the dislocation-vacancy mechanisms in the specimens.

8. Lomas, T. W., J. O. Ward, J. R. Reit, and E. W. Colbeck, "The Influence of Frequency of Vibration on the Endurance Limit of Ferrous Alloys at Speeds up to 150,000 Cycles per Minute Using a Pneumatic Resonance System", Proceedings of the International

Conference on Fatigue of Metals, London, September 14, 1956, and New York, November 30, 1956, Institution of Mechanical Engineers, London, England, pp. 375-385.

A pneumatic resonance system was designed to compare the fatigue properties of wrought and cast turbine blades for airplane engines. This machine, which operated at frequencies as high as 2500 cps, consumed up to 200 cubic feet of compressed air per minute at a supply pressure of about 90 psi. The specimen to be tested was used as a reed to actuate a resonant column of air in a tube. Two methods were used for measuring stress: measuring strain directly with strain gages and calculating stress, and measuring the vibration amplitude with a telemicroscope and calculating the stress. Curves were plotted to show the effect of frequency on the endurance limit for four types of steel at 10^8 cycles.

9. Vidal, G., and F. Girard, "Sur un nouveau dispositif de rupture des matériaux par un effort alternatif sinusoidal à 87 000 c/s", Comptes Rendus, Academie des Sciences, Volume 243, 1956, pp. 1276-1278.

This fatigue testing device was driven by a barium titanate cylinder with a natural longitudinal frequency of 87 kc. Resonant cylindrical specimens were attached to the upper face of the barium titanate cylinder by means of a central flange. Cylindrical specimens, 3 mm in diameter, of aluminum alloy, titanium alloy, and glass were fractured with this device. Specimens of magnesium alloy and steel that were necked down on either side of the flange and specimens of glass that were lengthened on the upper end by a half-wave truncated cone were also fractured. The fractures appeared the same as those obtained at low frequency. None of the specimens showed noticeable heating during the tests.

10. Vidal, G., F. Girard, and P. Lanusse, "Sur un dispositif de rupture des métaux par un effort alternatif sinusoidal à haute fréquence", Comptes rendus, Academie des Sciences, Volume 242, 1956, pp. 986-988.

A device was developed for exerting a periodic axial force on a cylindrical specimen at frequencies in the order of 5000-8000 cps. A specimen was attached at one end to a dynamometer, which operated through extensometers, and at the other end to a laminated stack of nickel-iron alloy. The entire assembly was resonant at its fundamental frequency. A magnetic circuit, suitably amplified, induced an alternating emf which excited the assembly to resonance vibration with a considerable increase in load. With this apparatus, axial alternating forces as high as ± 230 kg were induced in the specimens. Steel cylinders of 4 mm^2 cross section were fractured at a frequency of 6000 cps, and Duralumin specimens of 10 mm^2 cross section were fractured at a frequency of 5380 cps. The fractures were similar to those obtained at low frequency. No noticeable heating of the specimens was observed.

11. Wade, A. R., and P. Grootenhuis, "Very High-Speed Fatigue Testing", Proceedings of the International Conference on Fatigue of Metals, London, September 14, 1956, and New York, November 30, 1956, Institution of Mechanical Engineers, London, England, pp. 361-369.

Fatigue tests were conducted on aluminum alloy bars with a variable-frequency torsional vibrator giving sinusoidal excitation of adequate power. The specimens were 1/8 inch square and ranged in length from 2.58 to 8.35 inches. The maximum amplitude, measured by a microscope, occurred at the ends of each specimen. The maximum input power was 1000 watts, and the operating frequencies used were 24, 370, 850, 1550, and 3835 cps. Curves were plotted to show the relationship between stress and the number of cycles to failure, stress and the number of hours to failure, speed and the number of hours to failure, and speed and fatigue strength. Cracks formed in most specimens at or near the center, and the variation in stress at the fracture was less than 2 percent of the maximum stress at the center.

1957

12. Brosens, P. J., R. W. Reid, and T. P. Rona, "Magnetostrictive Drive Techniques for Fatigue Testing of Metals Above 10 Kilocycles", WADC Technical Report 57-438, Massachusetts Institute of Technology, Cambridge, Massachusetts, Contract AF 33(616)-3233, December 1957.

A magnetostrictive exciter was constructed that operated at about 12 kc with approximately 1 kva of electrical input power. This exciter was intended to serve as a source for alternating stress in typical turbine blades in order to investigate fatigue failure in the blades. It soon became apparent that the exciter could not satisfy the requirements of intensive specimen testing and correlation of results. A light modulation technique for determining the amplitude of vibration was developed successfully. The report covered detection and calibration methods, the analytical and experimental approach to the impedance matching problem between source and load, and the use of existing equipment to trace fatigue development by frequency and damping measurements. It also evaluated other methods of excitation.

1958

13. Atawani, J., and H. Miyamoto, "Fatigue Tests of Metals at Ultrasonic Frequency", Transactions, Japan Society of Mechanical Engineers, Volume 24, 1958, pp. 480-483.

"A testing equipment and measurements are reported of the fatigue of metals under supersonic frequency. This equipment has an advantage over conventional fatigue machines in that stress alternations up to 10^8 reversals can be made within an hour or so. At the resonant condition, metal samples are subjected to alternating stresses above the fatigue limit by means of a magnetostriction transducer through an exponential brass horn. By this method the fatigue properties of various metals were investigated. To avoid temperature rise of the samples, water cooling was necessary. Under insufficient cooling, it was not possible to obtain large motions and high strains, presumably due to the increase of internal damping in the samples. Even marks in the most strained part of the samples, such as might be made by a very light scratch with a knife edge, had a considerable effect on the fatigue limit." (Author abstract)

14. Mason, W. P., "Internal Friction, Plastic Strain and Fatigue in Metals and Semiconductors", Monograph No. 3326, Bell Telephone System Technical Publications, 1958.

"By using a barium titanate driver attached to a tapered brass horn, containing a specimen of metal, it is possible to stress the specimen to fatigue failure. The internal friction and plastic strain of the specimen can be measured from the ratio of the driving voltage to the pickup voltage from the titanate and from the resonant frequency. It is found that there are two amplitude ranges for which the internal friction and plastic strain vary with stress. The final phase for metals results in a very rapid rise in internal friction and plastic strain, and ends in fatigue failure. The effect of a static stress is to increase the stiffness of metals for small alternating stress amplitudes and to lower the value of the alternating stress required to produce fatigue failure. Germanium is not subject to fatigue failure in the manner of a metal but suffers brittle fracture. A theory based on the action of Frank-Read dislocation loops is shown to agree with the measured results. Fatigue stresses can be increased by metallurgical treatments which reduce the lengths of the Frank-Read sources." (Author abstract)

15. Stephenson, N., "A Review of the Literature on the Effect of Frequency on the Fatigue Properties of Metals and Alloys", Memorandum No. M. 320, National Gas Turbine Establishment, Ministry of Supply, England, June 1958.

A number of the references cited indicated that fatigue limits increased as frequencies at which fatigue testing was conducted increased. Most of the literature reported work at low frequencies, 150 to 30,000 cpm, although some work at frequencies ranging from 30,000 to 1,000,000 cpm was reported. When materials susceptible to corrosion fatigue were tested in dry air, investigators found that fatigue limits were

appreciably greater than the corresponding values for tests in ordinary air. In two papers it was reported that damping capacity and dynamic modulus were dependent on frequency at stresses above the dynamic proportional limit. Another study on the effect of frequency (6000 and 20,000 cpm) on deformation characteristics shown by polished surfaces of pure aluminum indicated that marked disturbance was produced near grain boundaries and that a fine network structure was present within the grains. The striations that formed at the higher frequency frequently resulted in a granular surface film that gave a slightly stained appearance to the surface.

1959

16. Girard, F., and G. Vidal, "Micromachine de fatigue en traction-compression a 92,000 alternances par second", Revue de Métallurgie, Volume 56, 1959, pp. 25-39

A fatigue testing machine operating at 87,500 cps consisted of a barium titanate cylinder to which a cylindrical specimen was attached at a central flange of the specimen, constituting a nodal point. The maximum stress obtainable at 1-micron amplitude was 36 kg/mm^2. This device was effective in fracturing aluminum alloy, titanium alloy, and glass cylinders, but not cylinders of half-hard steel, brass, or magnesium alloy. The differences in breaking capabilities were attributed to differences in damping capacity of the various metals. The fatigue cracks resembled those obtained in low-frequency fatigue.

A similar device operating at 92,000 cps was used to test cylindrical-toroidal specimens. Duralumin specimens were fractured at 2-3 billion cycles at a stress level of 14 kg/mm^2. At 10^9 cycles the breaking stress was 16 kg/mm^2, while in ordinary low-frequency tests the maximum stress at the same number of cycles was stated to be 12 kg/mm^2. Such a fatigue test for light alloys permitted shortening the test time for 3×10^9 cycles from the usual 100 days-3 years to 8 hours.

17. Neppiras, E. A., "Metal Fatigue at High Frequency", Proceedings of the Physical Society, London, Volume 70B, 1959, pp. 303-401.

A magnetostrictive transducer and three exponentially tapered couplers were used to investigate metal fatigue at high frequencies. A single-flange mounting system insured that tests were performed under zero static load conditions. The input power for the tests was approximately 1 kilowatt. Two types of brass samples were used: a straight rod, and a symmetrically tapered workpiece, 3/16 inch in diameter in the center and 3/8 inch at the ends. For cooling, a 1/16-inch hole was bored axially in the specimen and coupler to permit continuous water flow. In all samples, fracture occurred as a lateral crack near the point of maximum strain. Fatigue limits were calculated both by means

of S-N curves and by measuring the flow rate and temperature rise of the cooling water (to obtain the rate of energy loss). High-frequency testing permitted a normal fatigue run of 10^8 reversals in about 1.5 hours, compared to several weeks on conventional machines.

18. Neppiras, E. A., "Techniques and Equipment for Fatigue Testing at Very High Frequencies", Proceedings of the American Society for Testing Materials, Volume 59, 1959, pp. 691-709.

Resonant ultrasonic vibrators used in high-frequency fatigue testing consisting of a transducer, velocity transformer (coupler), and test specimen were described. The extensional, torsional, and flexural modes of operating the conventional types of electromechanical transducer (piezomagnetic, piezoelectric, and electrodynamic) were explained, and a study was made of the design of resonant velocity transformers and test specimens. Practical systems had been operated at frequencies above the audible limit, 18,000 to 22,000 cps. The advantages of ultrasonic testers were listed as: ease of operation; economy; variety of applications; and speedy, silent operation. Fatigue limits of metals at high frequency were reported to be seldom identical to those measured at low frequency, with discrepancies as high as 40 percent for brasses. Techniques for preventing overheating at high frequencies were described.

1960

19. Balalaev, Yu. F., "Structural Changes and Strength of Steel Under High-Frequency Cyclic Loading", Metallovedenie i Termicheskaya Obrabotka Metallov, April 1960, Number 4, pp. 41-45.

A resonance-type system was developed for investigating the fatigue strength, temperature effects from damping, and physiochemical processes under stresses at 17 to 20 kc at a maximum input power of 3 kva; the resonant length of the amplitude converter was 160 millimeters. The specimens were rods, 5 millimeters in diameter, of steel, copper, brass, aluminum alloy, and cast iron. High-frequency loading caused considerable heating of unhardened steel at the stress antinode from microplastic internal friction. An increase in frequency from 17.25 to 20 kc did not affect the fatigue limit of steel significantly. Microstructural changes were observed in the metals. Fatigue curves were constructed for iron and steel to approximately 10^7 cycles. The most efficient couplers used were those with an exponential or catenoidal shape.

20. Neppiras, E. A., "Very High Energy Ultrasonics", British Journal of Applied Physics, Volume 11, 1960, pp. 143-150.

Ultrasonic fatigue testing was included in a general survey of very-high-energy ultrasonics. The discussion dealt with fatigue testing

techniques rather than specific tests. The properties of piezomagnetic and piezoelectric transducer materials were outlined, and wave equations for conical, exponential, catenoidal, and double-quarter-wave cylindrical couplers were presented. Typical specimens were of symmetrically tapered and dumbbell shapes. The use of S-N curves to plot stress data was described and illustrated for alloy specimens at 18 kc to approximately 10^8 cycles. Endurance limits at high frequencies were somewhat higher than those for low frequencies; no satisfactory explanation was presented.

1961

21. Atawani, J., "Fatigue Tests of Metals at Ultrasonic Frequency. 2nd Report: For Materials Having High Endurance Limits", Bulletin of the Japan Society of Mechanical Engineers, Volume 4, 1961, pp. 466-470.

A fatigue tester was used to produce fundamental vibration in a dumbbell-shaped specimen, which was designed to induce highest stress in the contracted midportion. Analysis of vibration of the specimen at resonance condition was developed, and the results were confirmed by experiments with bearing steel specimens at a frequency of 18.3 kc. S-N curves showed a fatigue limit at about 10^8 stress reversals at 40 kg/mm^2, a higher number of stress reversals, and a lower value of stress than was expected for this material. The slope of the curve was steep. With an untapered copper specimen, the breaking stress at 10^8 reversals was about 8 kg/mm^2, practically the value expected from ordinary measurement.

22. Van Leeuwen, H. P., and M. C. Mucuoglu, "Requirements for an Axial Fatigue Machine Capable of Fast Cyclic Heating and Loading", AGARDograph 66 (amended edition), Advisory Group for Aeronautical Research and Development, Paris, France, September 1961.

Among other fatigue testing devices, the magnetostriction fatigue machine built by Neppiras in England was described briefly. Its salient features were a laminated dumbbell-type magnetostrictive transducer and a resonant tapered coupler. The specimen, which was approximately resonant at the transducer frequency, was tapered from a diameter at the center of 3/16 inch to 3/8 inch at the ends. The specimens had a hole 1/16 inch in diameter lengthwise through the middle to provide for water cooling. The machine had a loading capacity of 300 kg and was operated at speeds as high as 10^6 cpm. Distribution curves were constructed to show particle motion and stress in the mechanical transmission line.

1962

23. Grootenhuis, P., and P. Benham, "Vibration and Fatigue", Discovery, Volume 23, May 1962, pp. 36-43.

Both the slow, high-stress reversals that can cause metal failure after only a few hundred cycles and the high-speed, low-stress vibrations that may continue for millions of cycles before ultimate fracture were discussed. Work previously reported for both low- and high-frequency fatigue testing was reviewed. The failures at high stress were found to be most common when a component was subjected to a starting-and-stopping cycle. In aircraft particularly, the trend toward higher speeds has subjected components to vibrations at higher frequencies, so that components have more often been vibrated at their resonant frequencies and therefore at higher stresses. Long-endurance fatigue is usually associated with a sinusoidal cycle and frequencies of several thousand cycles per minute. With high-frequency fatigue, stressing is applied continuously at very high speed for a very great number of cycles and results in a shorter time lapse before failure.

24. Van Houten, J. J., "High Intensity Sonic Testing--A Tool for the Structural Analyst", Symposium on Shock, Vibration and Associated Environments, Part II, Washington, D. C., October 1-4, 1962, pp. 181-188.

The testing machine described made use of four electropneumatic transducers and exponential couplers, 6 feet long, with a frequency range from 40 to 3000 cps, and power output up to 2000 acoustical watts. Acoustical power was calculated by measuring sound pressure across the tube and converting these measurements to intensity in watts per square centimeter.

1963

25. Clifton, T. E., B. S. Hockenhull, and A. R. Sollars, "The Development and Evaluation of an Ultrasonic Fatigue Unit", Note No. 141, The College of Aeronautics, Cranfield, England, March 1963.

A fatigue test unit operating at 20 kc consisted of a magnetostrictive transducer and a half-wave velocity transformer with an amplification ratio of 6.25 to 1; the transformer was supported by a nodal flange, and dumbbell-type specimens were screw-attached to its smaller end. Temperature measurements at the highest stress level indicated that the temperature rose by less than 1°C over a period of 300 seconds. The addition of a cycle counter permitted accurate measurement of the number of cycles to failure. In initial tests with aluminum alloys, the results proved to be

highly sensitive to the surface finish on the specimens, and subsequent specimens were electrolytically polished before tests. In comparison with results obtained with a 200-cps rotating-bend machine, the higher frequency showed substantially higher stress levels throughout the S-N curve. Because of this frequency effect, it was concluded that application of the equipment to accelerated evaluation tests may not be simple.

1964

26. Brown, B., "High Intensity Ultrasonics", Industrial Electronics, March 1964, pp. 113-116.

Various high-power applications of ultrasonics were reviewed. Discussion was presented of the acceleration of fatigue testing, especially when specimens must be subjected to 10^8 stress reversals, by operating at ultrasonic frequencies. Basic equipment consisted of a 20-kc magnetostrictive transducer and a velocity transformer attached to the specimen under test. Large-amplitude vibration could thus be transmitted to the specimen even with the transducer operating under low stress. A maximum power of 60 watts was supplied to the transducer.

27. Skipnichenko, A. L., "The Use of Ultrasonic Vibration in Fatigue Tests", Zavodskaya Laboratoriya, Volume 30, 1964, pp. 598-599..

A method was presented for determining the effect of a cyclic load on the mechanical properties of metals. Cyclic loading was accomplished at an alternating stress of 17.5 kg/mm^2, using a 20.2-kc magnetostrictive transducer and a tapered velocity transformer screw-attached to a resonant annealed copper specimen. Since the central portion of each specimen became extremely hot during the tests, it was externally cooled by running water. With increased duration of the test, yield and ultimate tensile strength and hardness increased, while elongation decreased. The final failure took place after 110-125 seconds.

28. Thiruvengadam, A., "High Frequency Fatigue of Metals and Their Cavitation Damage Resistance", Technical Report 233-6, Hydronautics, Incorporated, Laurel, Maryland, Navy Contract Nonr-3755 (00) FBM, December 1964.

High-frequency fatigue tests were carried out on aluminum, bronze, Monel, and stainless steel by using a 14.2-kc magnetostrictive apparatus to drive notched specimens in resonance. Analysis of the results indicated that the high frequency did not significantly change the plastic energy required to fracture the metals in fatigue. Strain energy was correlated with cavitation damage resistance. High-frequency fatigue was significantly accelerated in a corrosive environment.

1965

29. Balalaev, Yu. F., "High Temperature Failure of Metals Under the Action of Ultrasonic Vibrations", Fizika Metallov i Metallovedenie, Volume 19, 1965, pp. 735-740.

Magnetostrictive apparatus operating at 24-26 kc was used to fatigue several materials without cooling, to determine the effect of internal friction heating on microstructure and fatigue fracture. Failure in aluminum and iron was accompanied by necking, presumed to be assisted by recovery, recrystallization, substructure formation, grain-boundary migration, and healing of micropores at cavities. Copper, steel, and high-nickel alloys did not neck down, but failed from the generation and propagation of cracks, chiefly along grain boundaries. Temperatures at failure were within the range of 300-1400°C.

30. Fox, A., "A Comparison of Ultrasonic and Conventional Axial Fatigue Tests on Aluminum Alloy Rod", Materials Research and Standards, February 1965, pp. 60-63.

Results obtained from conventional (60 cps) and ultrasonic (17.5 kc) axial-load fatigue tests on dumbbell-shaped rods of aluminum alloy were compared. In the ultrasonic test, longitudinal vibrations were induced in the test specimen by means of a barium titanate transducer and an exponentially tapered coupler. The ultrasonic method used required a specimen of relatively small diameter (0.125 inch necked down to 0.052 inch) because of the power limitations and the small amplitude of vibration. The specimen used for the conventional test was 0.438 inch in diameter necked down to 0.100 inch, and alignment of the specimen was very critical. A fatigue strength of approximately ± 14,000 psi at 10^8 stress reversals was obtained in both tests. The accuracy of the ultrasonic data was estimated at ± 12 percent because of the small specimen cross section. It was suggested that a more powerful transducer capable of vibrating a larger mass at greater amplitude be used for more accurate determinations.

31. Honeycutt, C. R., and J. C. Sawyer, "Determination of Elevated-Temperature Fatigue Data on Refractory Alloys in Ultra-High Vacuum", TRW Equipment Group, TRW, Inc., Cleveland, Ohio, NASA Contract NAS 3-6010: CR 54203, First Quarterly Report, July-September 1964; CR 54286, Second Quarterly Report, October-December 1964; CR 54389, Third Quarterly Report, January-March 1965; CR 54458, Fourth Quarterly Report, April-June 1965; CR 54775, Fifth Quarterly Report, July-September 1965; CR 54916, Sixth Quarterly Report, October 1965-January 1966.

Refractory metal alloys were subjected to high-frequency fatigue at temperatures up to 3000°F in ultrahigh vacuum, using a 20-kc hollow cylindrical transducer of lead titanate zirconate attached to stepped titanium couplers. The specimens were dumbbell-shaped, both smooth and notched. Successful tests were made with notched specimens, but sufficient stress could not be induced in smooth specimens of TZC and TZM molybdenum alloy to cause failure, even at 7.3×10^{11} cycles (503 hours).

APPENDIX II

DESIGN OF SAMPLE CONFIGURATION

Consider a sample configuration of the general type as shown in the sketch below:

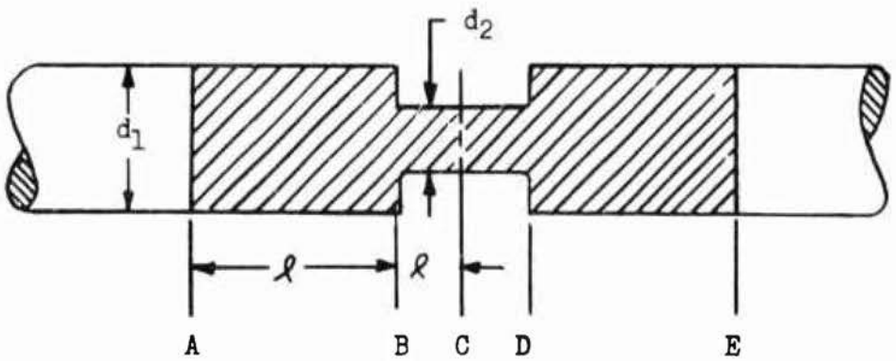

A schematic design of the overall sample to be tested is of the general configuration as shown between A and E. The sample is rigidly connected to a driving coupler from the transducer at A. This point is acoustically established as an antinode in the longitudinal vibration pattern of the system, and for the purpose of this analysis we will disregard any acoustic impedance mismatching occurring at the interfaces A or E. The section BD is the actual test section of the specimen, and it is desired to maximize the vibratory stress in this region. Unwanted stress concentration will be minimized by appropriate design.

Let ξ_x represent the longitudinal vibration amplitude occurring at any point along the test specimen. A general expression for the variation of ξ_x with respect to position and time is given by

$$\xi_x = \xi_0 \cos kx \sin \omega t, \qquad (3)$$

where ξ_0 = maximum longitudinal vibration amplitude,

$k = 2\pi/\lambda = \omega/c$

λ = wavelength

c = velocity of sound

$\omega = 2\pi f$

f = vibrational frequency

x = longitudinal coordinate

t = time.

Since we are interested only in the maximum values of ξ_x with respect to time, we can omit the time-dependent term and write

$$\xi_x = \xi_0 \cos kx. \tag{4}$$

The strain corresponding to this displacement is given by

$$\left(\frac{\partial \xi}{\partial x}\right) = -k\ \xi_0 \sin kx. \tag{5}$$

At point B in the figure, assuming the origin to lie at point A, the quantities are given by

$$\xi_B = \xi_0 \cos k\ \ell_1\ , \tag{6}$$

$$\left(\frac{\partial \xi}{\partial x}\right)_B = -k\ \xi_0 \sin k\ \ell_1. \tag{7}$$

Considering these quantities in the reduced section BD, it is convenient to take an origin at the center, C, and define values of x to the left of C as positive.

If we set the position of maximum strain in the reduced section to be at this origin, then the following expressions hold:

$$\xi' = \xi'_0 \sin k\ x'\ , \tag{8}$$

$$\left(\frac{\partial \xi}{\partial x}\right)' = k\ \xi'_0 \cos k\ x'\ , \tag{9}$$

where the primed quantities indicate the second coordinate system, and at position B,

$$\xi'_B = \xi'_0 \sin k\ \ell_2\ , \tag{10}$$

$$\left(\frac{\partial \xi}{\partial x}\right)'_B = k\ \xi_0 \cos k\ \ell_2\ . \tag{11}$$

One of the boundary conditions at plane B is that the particle displacements be equal in both sections. Thus,

$$\xi_B = \xi_B' \quad , \tag{12}$$

which, when combined with Equations (6) and (10), gives

$$\xi_B = \xi_o \frac{\cos k \ell_1}{\sin k \ell_2} \quad . \tag{13}$$

This expression gives the amplification of particle displacement occurring in the test section.

The second boundary condition at plane B is that the forces exerted by the two sections be equal and opposite in sign. Thus,

$$-F_B = F_B' \quad . \tag{14}$$

Force is related to strain by the general expression

$$F = A E \frac{\partial \xi}{\partial x} \quad , \tag{15}$$

where A is the cross-sectional area and E is the modulus of elasticity.

Utilising Equations (7) and (11) and assuming E to remain constant throughout the test piece at any specified operating frequency, then the following equation is obtained:

$$\frac{d_1^2}{d_2^2} = \cot k \ell_1 \cot k \ell_2 \quad . \tag{16}$$

Equation (16) therefore gives the relationship between the dimensions of the test shape to provide maximum vibratory stress in the test region of the specimen.

APPENDIX III

FORCE-INSENSITIVE MOUNTING SYSTEM

Effective transmission of high-frequency vibratory energy into a system under load, as in the complex fatigue-loading system herein described, invariably demands the use of force-insensitive mounting systems. Such systems have been developed in our laboratory (reference 2) and have been routinely used in a variety of ultrasonic systems.

The application of force through a conventional transducer-coupling system has two adverse effects on the efficiency of the system: (1) the system resonant frequency may shift to such an extent that matching or tracking of the frequency with the frequency converter may be difficult or impractical, and (2) substantial amounts of energy may be lost to the mounting system so that little is delivered to the work area.

The damping phenomenon is readily comprehended from an examination of known acoustic transmission principles. If a rod is acoustically excited in the longitudinal mode at a resonant frequency and if no acoustic energy is transmitted out of the rod, a standing-wave pattern is set up in the rod; under these conditions the rod can be supported at nodal points (points of no longitudinal particle motion) with no appreciable loss of energy. However, as soon as the rod is coupled into a medium which will allow transmission of acoustic energy through the rod without complete reflection at the radiating face, the energy is delivered to the medium in traveling or progressive waves, and there are no nodal points associated with the delivered energy. In the case of complete transmission, the particle wave pattern becomes a traveling wave with maximum particle displacements occurring all along the rod. In any case involving the delivery of vibratory energy, mounting the transmission rod at a so-called nodal point results in loss of acoustic energy to the supporting members.

When static force is applied to such a system, particle motion is restrained and even further loss of energy occurs. In connection with ultrasonic impact drilling, for example, the transducers have been noted to "stall" when loads of more than a few pounds are applied (reference 5). Obviously such an arrangement is ineffective for such operations as machining, forging, drawing, extrusion, and the like, where forces of high magnitude are essential.

The force-insensitive mounting systems which we have developed make it possible to mount a transmission system rigidly without loss of acoustic energy to the supporting structure and without changing the resonant frequency of the system. The force-insensitive mount is, in essence,

a member surrounding and metallurgically attached to the transmitting coupler, which is an integral number of half wavelengths long. One end of the sleeve is affixed to the coupler while the other end is free, providing a couple into air, as shown in Figure 17.

The high impedance of this sleeve into air results in negligible energy transmission, practically complete wave reflection, and a true standing-wave pattern in the sleeve, so that there is an absolute nodal point one quarter-wavelength from the end where a rigid mounting flange can be affixed without loss of energy, even when high loads are applied.

This arrangement has the further advantage of providing a means for hermetically sealing the transducer-coupling system through the walls of any type of chamber, so that energy can be effectively transmitted into high-pressure, high-temperature, corrosive, or inert atmospheres.

Such systems are routinely used in ultrasonic welding equipment in which several hundred pounds of force are applied. They have been used in powder compaction systems which have involved loads of more than 100 tons. Evaluation of one such system indicated a frequency deviation of no more than 2 percent under loads up to 80 tons.

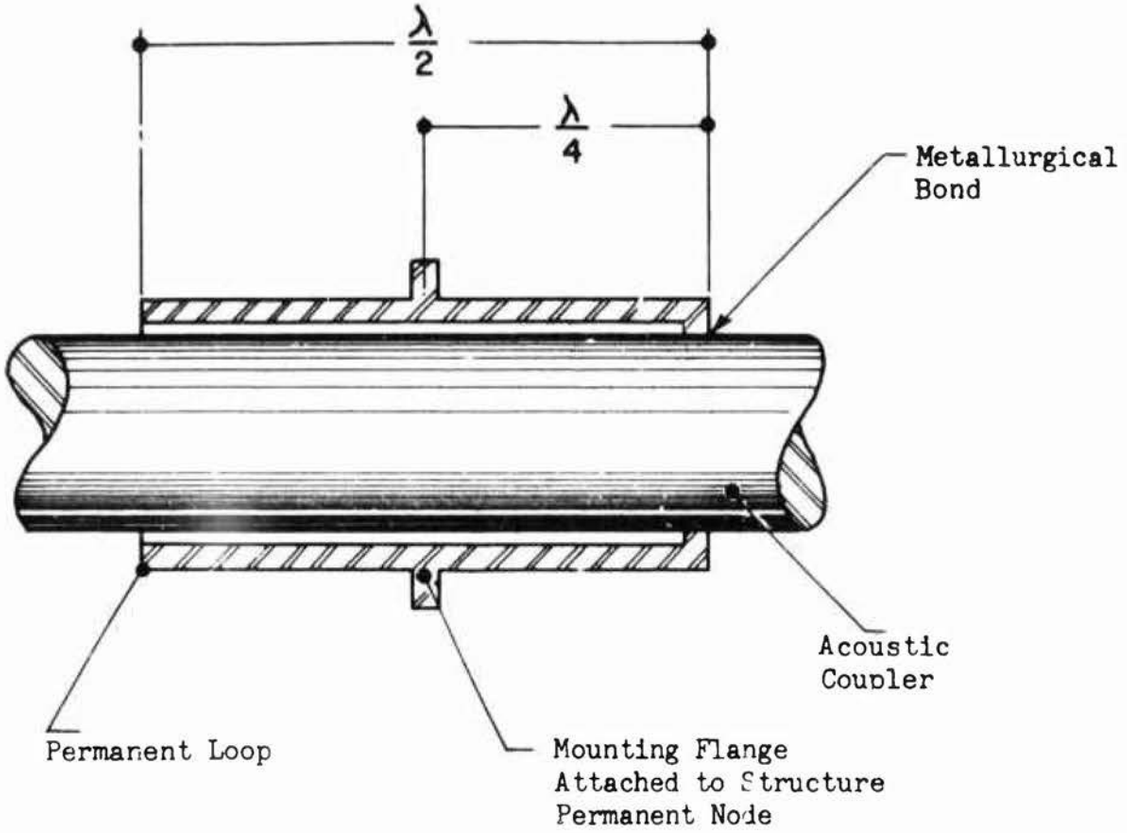

Figure 17. Force-Insensitive Mounting Device.

DISTRIBUTION

US Army Materiel Command	3
US Army Aviation Materiel Command	6
Chief of R&D, DA	1
Director of Defense Research and Engineering	1
US Army R&D Group (Europe)	2
US Army Aviation Materiel Laboratories	24
US Army Engineer R&D Laboratories	2
US Army Limited War Laboratory	1
US Army Ballistic Research Laboratories	2
US Army Research Office-Durham	1
Plastics Technical Evaluation Center	1
US Army Engineer Waterways Experiment Station	1
US Army Test and Evaluation Command	1
US Army Electronics Command	2
US Army Combat Developments Command Transportation Agency	1
US Army Aviation School	1
US Army Tank-Automotive Center	2
US Army Aviation Test Board	2
Air Force Flight Test Center, Edwards AFB	1
Air Force Flight Dynamics Laboratory, Wright-Patterson AFB	1
Systems Engineering Group, Wright-Patterson AFB	2
Naval Air Systems Command, DN	4
Office of Naval Research	1
US Naval Research Laboratory	1
Commandant of the Marine Corps	1
Marine Corps Liaison Officer, US Army Transportation School	1
Lewis Research Center, NASA	1
NASA Scientific and Technical Information Facility	2
NAFEC Library (FAA)	2
National Tillage Machinery Laboratory	1
US Army Board for Aviation Accident Research	1
Bureau of Safety, Civil Aeronautics Board	2
US Naval Aviation Safety Center, Norfolk	1
Federal Aviation Agency, Washington, D. C.	2
US Army Medical R&D Command	1
US Government Printing Office	1
Defense Documentation Center	20

UNCLASSIFIED
Security Classification

DOCUMENT CONTROL DATA · R&D

(Security classification of title, body of abstract and indexing annotation must be entered when the overall report is classified)

1. ORIGINATING ACTIVITY (Corporate author) AEROPROJECTS INCORPORATED WEST CHESTER, PENNSYLVANIA	2a. REPORT SECURITY CLASSIFICATION UNCLASSIFIED 2b GROUP

3. REPORT TITLE

DEVELOPMENT OF EQUIPMENT AND TECHNIQUES FOR COMPLEX FATIGUE LOADING

4. DESCRIPTIVE NOTES (Type of report and inclusive dates)

Final Technical Report

5. AUTHOR(S) (Last name, first name, initial)

Kartluke, Herbert
Luckhardt, Philip L.
Pruder, Gary D.

6. REPORT DATE	7a. TOTAL NO. OF PAGES	7b. NO. OF REFS
December 1966	75	9

8a. CONTRACT OR GRANT NO.	9a. ORIGINATOR'S REPORT NUMBER(S)
DA-44-177-AMC-257(T) b. PROJECT NO. Task 1P125901A17002 c. d.	USAAVLABS Technical Report 66-86 9b. OTHER REPORT NO(S) (Any other numbers that may be assigned this report)

10. AVAILABILITY/LIMITATION NOTICES

Distribution of this document is unlimited.

11. SUPPLEMENTARY NOTES	12. SPONSORING MILITARY ACTIVITY
	U. S. Army Aviation Materiel Laboratories Fort Eustis, Virginia

13. ABSTRACT

Fatigue testing apparatus for simultaneous application of high-frequency, low-frequency, and static loading was designed and constructed. The equipment provided for the introduction of high-frequency vibratory energy at 15,000 cycles per second at one end of a specimen, and static loading and low-frequency vibration at 2000 cycles per minute at the opposite end. Specimens with a necked-down test section were designed for resonance at the high frequency, and the specimen holding arrangement insured effective delivery of the high-frequency energy into the specimen.

The feasibility of the apparatus as a fatigue test instrument was demonstrated in limited tests on integral specimens of 4340 steel, 2014-T6 aluminum alloy, and 6Al-4V titanium alloy, and on joint specimens of 4340 steel involving fusion-welded, riveted, adhesive-bonded, and brazed joints. With constant low-frequency and static loads, the specimens generally demonstrated shorter elapsed time to failure as the high-frequency power input was increased. The titanium alloy, however, appeared to be insensitive to the high-frequency vibration at the power levels used, possibly because of its internal hysteresis characteristics.

The equipment provides a means for laboratory testing of materials and joint designs for knowledge of materials behavior under conditions encountered in rocket-propelled vehicles. It was recommended that comprehensive fatigue testing be carried out with this apparatus and that methodology be evolved for evaluation and use of the test data.

DD FORM 1 JAN 64 1473

UNCLASSIFIED
Security Classification

14 KEY WORDS	LINK A		LINK B		LINK C	
	ROLE	WT	ROLE	WT	ROLE	WT

INSTRUCTIONS

1. ORIGINATING ACTIVITY: Enter the name and address of the contractor, subcontractor, grantee, Department of Defense activity or other organization *(corporate author)* issuing the report.

2a. REPORT SECURITY CLASSIFICATION: Enter the overall security classification of the report. Indicate whether "Restricted Data" is included. Marking is to be in accordance with appropriate security regulations.

2b. GROUP: Automatic downgrading is specified in DoD Directive 5200.10 and Armed Forces Industrial Manual. Enter the group number. Also, when applicable, show that optional markings have been used for Group 3 and Group 4 as authorized.

3. REPORT TITLE: Enter the complete report title in all capital letters. Titles in all cases should be unclassified. If a meaningful title cannot be selected without classification, show title classification in all capitals in parenthesis immediately following the title.

4. DESCRIPTIVE NOTES: If appropriate, enter the type of report, e.g., interim, progress, summary, annual, or final. Give the inclusive dates when a specific reporting period is covered.

5. AUTHOR(S): Enter the name(s) of author(s) as shown on or in the report. Enter last name, first name, middle initial. If military, show rank and branch of service. The name of the principal author is an absolute minimum requirement.

6. REPORT DATE: Enter the date of the report as day, month, year; or month, year. If more than one date appears on the report, use date of publication.

7a. TOTAL NUMBER OF PAGES: The total page count should follow normal pagination procedures, i.e., enter the number of pages containing information.

7b. NUMBER OF REFERENCES: Enter the total number of references cited in the report.

8a. CONTRACT OR GRANT NUMBER: If appropriate, enter the applicable number of the contract or grant under which the report was written.

8b, 8c, & 8d. PROJECT NUMBER: Enter the appropriate military department identification, such as project number, subproject number, system numbers, task number, etc.

9a. ORIGINATOR'S REPORT NUMBER(S): Enter the official report number by which the document will be identified and controlled by the originating activity. This number must be unique to this report.

9b. OTHER REPORT NUMBER(S): If the report has been assigned any other report numbers *(either by the originator or by the sponsor)*, also enter this number(s).

10. AVAILABILITY/LIMITATION NOTICES: Enter any limitations on further dissemination of the report, other than those imposed by security classification, using standard statements such as:

(1) "Qualified requesters may obtain copies of this report from DDC."

(2) "Foreign announcement and dissemination of this report by DDC is not authorized."

(3) "U. S. Government agencies may obtain copies of this report directly from DDC. Other qualified DDC users shall request through _____."

(4) "U. S. military agencies may obtain copies of this report directly from DDC. Other qualified users shall request through _____."

(5) "All distribution of this report is controlled. Qualified DDC users shall request through _____."

If the report has been furnished to the Office of Technical Services, Department of Commerce, for sale to the public, indicate this fact and enter the price, if known.

11. SUPPLEMENTARY NOTES: Use for additional explanatory notes.

12. SPONSORING MILITARY ACTIVITY: Enter the name of the departmental project office or laboratory sponsoring *(paying for)* the research and development. Include address.

13. ABSTRACT: Enter an abstract giving a brief and factual summary of the document indicative of the report, even though it may also appear elsewhere in the body of the technical report. If additional space is required, a continuation sheet shall be attached.

It is highly desirable that the abstract of classified reports be unclassified. Each paragraph of the abstract shall end with an indication of the military security classification of the information in the paragraph, represented as *(TS), (S), (C), or (U)*.

There is no limitation on the length of the abstract. However, the suggested length is from 150 to 225 words.

14. KEY WORDS: Key words are technically meaningful terms or short phrases that characterize a report and may be used as index entries for cataloging the report. Key words must be selected so that no security classification is required. Identifiers, such as equipment model designation, trade name, military project code name, geographic location, may be used as key words but will be followed by an indication of technical context. The assignment of links, rules, and weights is optional.